DOE/ET-53088-116 IFSR #116

THEORY OF ANOMALOUS TEARING MODE GROWTH AND THE MAJOR TOKAMAK DISRUPTION

P. H. Diamond, R. D. Hazeltine, and Z. G. An
Institute for Fusion Studies

B. A. Carreras
Oak Ridge National Laboratory

H. R. Hicks
Union Carbide Corporation

January 1984

Theory of Anomalous Tearing Mode Growth and the Major Tokamak Disruption

P. H. Diamond, R. D. Hazeltine, and Z. G. An
Institute for Fusion Studies, University of Texas, Austin, Texas 78712

B. A. Carreras
Oak Ridge National Laboratory, Oak Ridge, Tennessee 37830

H. R. Hicks
Computer Sciences, Union Carbide Corporation, Nuclear Division,
Oak Ridge, Tennessee 37830

ABSTRACT

An analytic theory of turbulence in reduced resistive magnetohydrodynamics is developed and applied to the major disruption in tokamaks. The renormalized equations for a long wavelength tearing instability are derived. The theory predicts two principal nonlinear effects: an anomalous flux diffusivity due to turbulent fluid convection in Ohm's law and a vorticity damping term due to turbulent magnetic stresses in the equation of motion. In the final phase of the disruption, when fine-scale fluid turbulence has been generated, detailed considerations show that anomalous diffusivity has the dominant effect at long wavelengths.

For a low m tearing mode, the solution of the renormalized equations during the turbulent phase yields a growth rate analogous to the classical case but increased by turbulent resistivity: $\gamma \sim (\sum_{\vec{k}'} k_\theta'^2 |\phi_{\underline{k}'}|^2)^{3/8} (\Delta')^{1/2}$. This analytical prediction is in good accord with computational results.

I. INTRODUCTION

Major disruptions place a serious limitation on tokamak performance.[1] Hence, it is crucial to develop detailed theoretical and computational models of the disruptive instability so that measures to control disruptions can be developed. Furthermore, the major disruption model[2] based on the nonlinear interaction of tearing modes[3] provides an excellent context for the study of strong resistive magnetohydrodynamic turbulence. In particular, an understanding of the major tokamak disruption from this viewpoint requires a satisfactory explanation of the effects of fully developed, small-scale, resistive magnetohydrodynamic turbulence on low-mode-number tearing instabilities and other macroscopic phenomena. Many numerical calculations of multiple-helicity tearing interactions[2] have been done with the aim of understanding the dynamics of this process. Effects such as resistivity evolution,[4] toroidicity,[5] noncircularity of the plasma cross section,[6] and diamagnetic rotation[7] (ω_*) have been included. It has been shown that they do not modify the basic dynamical mechanism of the nonlinear interaction of tearing modes. Therefore, in the present paper the large aspect ratio, reduced set of resistive magnetohydrodynamic equations,[8] applied to cylindrical geometry will be considered. The numerical calculations have been done using an initial value approach, which, by appropriate choice of the initial conditions, permits the separation in time of a sequence of phenomena that constitute the basic dynamical mechanism of the major disruption model. They can be summarized as follows.

The initial equilibrium is linearly unstable to the (m=2; n=1) and (m=3; n=2) resistive tearing modes. Here, m and n are poloidal and toroidal mode numbers, respectively. These modes grow exponentially in time until the width of their magnetic islands becomes comparable to the width of the resistive tearing layer. Then the evolution of the instabilities enters the Rutherford phase[9] characterized by island growth which is linear with time. This reduction in growth rate is a consequence of the balance of the linear magnetic driving forces with nonlinear $\vec{J} \times \vec{B}$ forces, rather than with inertia. As the m/n = 2/1 and 3/2 magnetic islands grow larger, nonlinear coupling through the (m=5; n=3) mode, which tends to accelerate the growth of the (m=3; n=2) mode, occurs. Finally, the 2/1 and 3/2 islands overlap, resulting in the occurrence of stochastic magnetic field lines throughout most of the plasma volume. As the islands overlap, the rapid growth, characteristic of disruptive phenomena begins. The sequence of phenomena leading to the final disruptive phase is depicted in Fig. 1.

In the phase of rapid growth, three distinct processes can be distinguished. In the numerical calculations, these processes can be separated into sequential phases of the (m=3; n=2) mode behavior by choosing a very small initial width for this mode (Fig. 1). First,[10] following the overlap of the 2/1 and 3/2 magnetic island, the large current gradient that develops in the region between the two islands results in a positive Δ' for the nonlinearly driven (m=5; n=3) fluctuation. Here the nonlinear drive is a consequence of the overlap of the (m=2; n=1) and (m=3; n=2) modes. The resonant mode coupling of the (m=2; n=1) mode with the (m=5; n=3) mode then results in the rapid, nonlinear destabilization of the (m=3; n=2) mode. In particular, the

$\vec{J} \times \vec{B}$ force resulting from the beating of the (m=5;n=3) mode with the (m=2;n=1) mode drives a rapid increase in the kinetic energy of the (m=3;n=2) mode. The theoretical model advanced in Ref. 10 is in good agreement with the computational results during this phase.

The nonlinear interaction of the low m mode leads to the generation of large m turbulence. Following the generation of the short wavelength fluid turbulence is a rapid increase in the growth rate of the (m=3;n=2) mode. This corresponds to the final increase in γ_{32} in Fig. 1. Simultaneously, generation of large m turbulence proceeds at a rate comparable to the growth rate of this mode. During this final phase, poloidal flux is expelled, resulting in a change in the self-inductance of the plasma and a negative voltage spike. The voltage spike occurs at a rate comparable to the (m=3;n=2) growth rate. The plasma behavior during this phase of the calculation is insensitive to any variation in the collisional resistivity.[11]

In this paper, we will focus on the final phase of the major disruption. Preliminary results of this investigation have been presented in Ref. 12. The observed generation of short wavelength turbulence and the insensitivity of the dynamics to collisional resistivity strongly suggest that the (m=3;n=2) mode and voltage spike growth rates are determined by nonlinear processes. Hence, a renormalized theory for the tearing mode response function in reduced resistive magnetohydrodynamics[8] is developed. This theory treats the effect of large m turbulence on low m tearing modes. The principal result of the theory is the prediction of an anomalous flux diffusivity $D^A_{\underline{k}} = \sum_{\vec{k}'} k'^2_\theta \langle \Phi^2 \rangle_{\underline{k}'} \gamma^{-1}_{\underline{k}'}$ due to the turbulent convection of flux by fluid motion. The anomalous diffusivity increases rapidly as short

wavelength fluid turbulence is generated. The rapid increase of diffusivity, $D_{\underline{k}}^{A}$, correlates well with the onset of insensitivity to the collisional resistivity. Using $D_{\underline{k}}^{A}$ in place of the collisional resistivity in Ohm's law yields a nonlinear tearing mode growth rate of $\gamma \propto (\sum_{\vec{k}} k_\theta^2 \langle\Phi^2\rangle_{\underline{k}})^{3/8} (\Delta')^{1/2}$. When the $\langle\Phi^2\rangle_{\underline{k}}$ spectrum obtained from the numerical calculation is used to calculate γ, the growth rate prediction is in good agreement with both the (m=3;n=2) growth rate and voltage spike time scales observed in the calculation. In addition to the anomalous ohmic diffusivity, the magnetic fluctuations exert a stress on the fluid that is manifested as a vorticity damping term in the equation of motion. This effect opposes the growth of fluid vorticity. However, because the nonlinear growth rate γ is larger than the vorticity damping rate, the anomalous ohmic diffusivity is the dominant nonlinear effect.

Several points of theoretical interest emerge from the analysis. First, the turbulence acts as both a destabilizing and stabilizing agent. The anomalous ohmic diffusivity, $D_{\underline{k}}^{A}$, triggers a rapidly growing tearing instability. In this case, nonlinear effects enhance a basically linear instability process that extracts magnetic free energy from the equilibrium. The turbulent vorticity damping, $a_{\underline{k}}$, opposes the growth of fluid energy but cannot saturate the nonlinear tearing process. The simultaneous influence of both types of processes is necessary for building a satisfactory model of rapid, disruptive behavior. Second, the predictions of local theory are strongly modified by magnetic shear, inhomogeneity, and the presence of mixed helicities. Specifically, because of magnetic shear, the different orientations of fluctuations localized at different singular surfaces

spread the effects associated with the well-known nonlinear transfer[13,14] of mean square flux to long wavelength. In contrast, turbulent diffusion of flux appears as a local differential operator. Thus this process — the dominant nonlinear effect in Ohm's law — has significant impact near the singular surface of the tearing mode. Finally, because this investigation is concerned with nonstationary, growing turbulence, a detailed consideration of eddy damping[15] times is unnecessary. It should be noted that, while the fluid turbulence spectrum is not self-consistently calculated, the theory does treat the interaction of the tearing mode and the large m turbulence self-consistently. The mechanism for generating the large m turbulence involves the balance of incoherent emission from lower m modes with vorticity damping and resistive dissipation. This balance results in a cascade of energy to large m. We will discuss the details of the generation mechanism in a future publication.

A first attempt at an analytical theory of this turbulent phase of the tokamak disruptions was made by D. J. Tetreault.[16] Several important discrepancies exist between the results of this paper and the results given in Ref. 16. These differences will be discussed in detail in the following sections.

The remainder of this paper is organized in the following fashion. In Sec. II the general structure and properties of the renormalized theory of reduced resistive magnetohydrodynamic turbulence is presented in the simple context of infinite medium theory. The renormalized equations are discussed in Sec. III. In Sec. IV the renormalization procedure is applied to the relevant case of multiple-helicity turbulence in a sheared magnetic field. In Sec. V, the renormalized

tearing mode equations are solved and the nonlinear growth rate is calculated. The comparison with numerical results is made in Sec. VI. Finally, the conclusions of this paper are summarized in Sec. VII.

II. GENERAL STRUCTURE OF THE RENORMALIZED THEORY OF REDUCED RESISTIVE MAGNETOHYDRODYNAMIC TURBULENCE

In this section, the general structure and properties of the renormalized theory of reduced resistive magnetohydrodynamic turbulence are discussed in the context of determining the long wavelength response function. Attention is focused on the treatment of symmetries and conservation laws in the renormalized theory.

To facilitate an understanding of the basic nonlinear processes, the simple case of externally driven turbulence in an infinite, homogeneous plasma immersed in uniform magnetic field, $\vec{B}_0$, is considered first. In this case, for which a local analysis is permissible, growth results from an imbalance of external forces and dissipation. In Sec. IV, the basic theory is applied to the more realistic and complicated situation of multiple-helicity turbulence in a sheared magnetic field.

The reduced resistive magnetohydrodynamic equations are:[8]

$$\frac{\partial \Psi}{\partial t} + (\vec{\nabla}\Phi \times \hat{n}) \cdot \vec{\nabla}\Psi = \eta J - \frac{\partial \Phi}{\partial z} + F^M , \tag{1}$$

$$\frac{\partial U}{\partial t} + (\vec{\nabla}\Phi \times \hat{n}) \cdot \vec{\nabla}U - \mu\vec{\nabla}_\perp^2 U = (\vec{\nabla}\Psi \times \hat{n}) \cdot \vec{\nabla}J - \frac{\partial J}{\partial z} + F^K . \tag{2}$$

Equation (1) is the Ohm's law, which relates the inductive and electrostatic parallel electric fields to the current. Equation (2) is the equation of motion, relating the parallel component of vorticity to Reynolds and magnetic stresses. Here, Ψ is the poloidal flux function and Φ is the velocity stream function. The parallel current J and the

parallel component of the vorticity U are related to the poloidal flux and velocity stream functions by $J = \vec{\nabla}_\perp^2 \Psi$ and $U = \vec{\nabla}_\perp^2 \Phi$, respectively. The unit vector $\hat{n}$ is parallel to the magnetic field, $\vec{B}_0$, and z is the coordinate along $\hat{n}$. The perpendicular velocity and magnetic field are given by:

$$\vec{V}_\perp = \vec{\nabla}\Phi \times \hat{n} \tag{3}$$

and

$$\vec{B}_\perp / |\vec{B}_0| = -\vec{\nabla}\Psi \times \hat{n} \ . \tag{4}$$

Time is normalized to the poloidal Alfvén time, τ_{Hp}, and lengths are normalized to the plasma minor radius a. In this system of units, the resistivity η is proportional to $\eta_0(r)/S$, where $\eta_0(r)$ is a slowly varying dimensionless resistivity profile function and $S = \tau_R/\tau_{Hp}$ [$\tau_R = a^2/\eta(0)$ is the time for resistive diffusion across the plasma], and μ is the collisional viscosity. F^M and F^K represent the effect of external forcing that drives the evolution of poloidal flux and vorticity, respectively.

Fourier-decomposing the poloidal flux and stream function perturbations $\tilde{\Psi}$ and $\tilde{\Phi}$ according to

$$\begin{Bmatrix} \tilde{\Psi} \\ \tilde{\Phi} \end{Bmatrix} = \sum_{\vec{k}} \begin{Bmatrix} \Psi_{\underline{k}} \\ \Phi_{\underline{k}} \end{Bmatrix} \exp\left[i (\vec{k}_\perp \cdot \vec{x}_\perp + k_\parallel z) \right] \ , \tag{5}$$

one obtains the reduced resistive magnetohydrodynamic equations for the fluctuation with wave vector $\vec{k}$:

$$\frac{\partial \psi_{\underline{k}}}{\partial t} + \sum_{\vec{k}'} \left[\vec{k}_\perp \cdot (\vec{k}'_\perp \times \hat{n})\right](\phi_{-\underline{k}'}\psi_{\underline{k}''} - \psi_{-\underline{k}'}\phi_{\underline{k}''})$$
$$= -ik_\parallel \phi_{\underline{k}} - \eta k_\perp^2 \psi_{\underline{k}} + F^M , \tag{6}$$

$$\frac{\partial}{\partial t}(k_\perp^2 \phi_{\underline{k}}) + \mu k_\perp^4 \phi_{\underline{k}} + \sum_{\vec{k}'} \left[\vec{k}_\perp \cdot (\vec{k}'_\perp \times \hat{n})\right](k_\perp''^2 - k_\perp'^2)\phi_{-\underline{k}'}\phi_{\underline{k}''}$$
$$= -ik_\parallel k_\perp^2 \psi_{\underline{k}} + \sum_{\vec{k}'} \left[\vec{k}_\perp \cdot (\vec{k}'_\perp \times \hat{n})\right](k_\perp''^2 - k_\perp'^2)\psi_{-\underline{k}'}\psi_{\underline{k}''} + F^K . \tag{7}$$

Here $\vec{B}_0 = B_0\hat{z}$, $\vec{x}_\perp$ and $\vec{k}_\perp$ are the vector and wave vector components perpendicular to $\vec{B}_0$, and $\vec{k}'' = \vec{k} + \vec{k}'$.

The ultimate goal of this investigation is to understand tearing instability turbulence and disruptive behavior in tokamaks. Because disruptive behavior is characterized by rapid nonlinear growth of long wavelength tearing instabilities and short wavelength turbulence, it is appropriate to consider a driven, nonstationary turbulent system in which external forcing exceeds viscous and resistive damping. The corresponding situation in ordinary hydrodynamics would be one of an energy cascade driven by long wavelength stirring, which is in turn increasing exponentially in time. For such a system, the time dependence of $\psi_{\underline{k}}$ and $\phi_{\underline{k}}$ can be taken as $\exp(\gamma_{\underline{k}}t)$, where $\gamma_{\underline{k}}$ is, in general, amplitude-dependent.

Following standard procedures,[15,17] the renormalized response functions for Eqs. (6) and (7) are derived by iteratively substituting the fields $\psi_{\underline{k}}^{(2)}$ and $\phi_{\underline{k}}^{(2)}$ — driven by the direct beat interaction of the test mode $\vec{k}$ with background fluctuation $\vec{k}'$ — for $\psi_{\underline{k}''}$ and $\phi_{\underline{k}''}$. This procedure extracts the lowest-order piece of the nonlinearity that is phase-coherent with the test fluctuation at wave vector $\vec{k}$. The driven fluctuations $\psi_{\underline{k}}^{(2)}$ and $\phi_{\underline{k}}^{(2)}$ are determined by:

$$(\gamma'' + \eta k_\perp''^2)\, \psi_{\underline{k}''}^{(2)} + i k_\parallel''\, \phi_{\underline{k}''}^{(2)} = S_1 \,, \tag{8}$$

$$(\gamma'' + \mu k_\perp''^2)\, \phi_{\underline{k}''}^{(2)} + i k_\parallel''\, \psi_{\underline{k}''}^{(2)} = S_2 \,, \tag{9}$$

where $\gamma'' = \gamma_{\underline{k}} + \gamma_{\underline{k}'}$, and

$$S_1 = \left[\vec{k}_\perp \cdot (\vec{k}_\perp' \times \hat{n})\right](\phi_{\underline{k}'}\psi_{\underline{k}} - \phi_{\underline{k}}\psi_{\underline{k}'}) \,, \tag{10}$$

$$S_2 = k_\perp''^{-2}\left[\vec{k}_\perp \cdot (\vec{k}_\perp' \times \hat{n})\right](k_\perp^2 - k_\perp'^2)(\phi_{\underline{k}'}\phi_{\underline{k}} - \psi_{\underline{k}'}\psi_{\underline{k}}) \,. \tag{11}$$

Note that, as in the case of nonresonant quasi-linear diffusion, the rapid growth associated with $\gamma_{\underline{k}}$ and $\gamma_{\underline{k}'}$ eliminates the need for an eddy damping rate[15] for the driven $\vec{k}''$ fluctuation. Straightforward manipulation then yields:

$$\psi_{\underline{k}''}^{(2)} = \frac{L_{\underline{k}''}}{\gamma_\eta''}\left(S_1 - i\frac{k_\parallel''}{\gamma_\mu''} S_2\right), \tag{12}$$

$$\phi_{\underline{k}''}^{(2)} = \frac{L_{\underline{k}''}}{\gamma_\mu''}\left(S_2 - i\frac{k_\parallel''}{\gamma_\eta''} S_1\right), \tag{13}$$

where

$$\gamma_\eta'' = \gamma'' + \eta k_\perp''^2 \tag{14}$$

$$\gamma_\mu'' = \gamma'' + \mu k_\perp''^2 \tag{15}$$

$$L_{\underline{k}''} = \left(1 + k_\parallel''^2/\gamma_\eta''\,\gamma_\mu''\right)^{-1} \,. \tag{16}$$

The propagator $L_{\underline{k}''}$ includes the effects of resistivity and viscosity-modified field line bending due to the driven fluctuation. Equation (16) indicates that small $k_{\parallel}''$ driven fluctuations are dynamically favored and large $k_{\parallel}''$ fluctuations are proportionately reduced. Furthermore, anticipating later consideration of turbulence in a sheared magnetic field, where background ($\vec{k}'$) turbulent fluctuations are quasi-localized with small $k_{\parallel}'$ and where the region around the $k_{\parallel} = 0$ surface of the test mode is of primary interest, it is assumed that the parallel wave vector distribution of the forcing functions, $F_{\underline{k}}^{K}$ and $F_{\underline{k}}^{M}$, is sharply peaked around $k_{\parallel} = 0$. Hence, $k_{\parallel}'' \ll \gamma_{\eta}''$, γ_{μ}'' are adopted hereafter, and it then follows that

$$\psi_{\underline{k}}^{(2)} \cong \frac{L_{\underline{k}''}}{\gamma_{\eta}''} S_1 \tag{17}$$

and

$$\phi_{\underline{k}}^{(2)} \cong \frac{L_{\underline{k}''}}{\gamma_{\mu}''} S_2 \, . \tag{18}$$

The renormalized response fluctuation can be simplified by noting that the structure of the nonlinear reduced resistive magnetohydrodynamic equations implies that one can impose

$$\psi_{-\underline{k}} = \psi_{\underline{k}} \tag{19}$$

and

$$\phi_{-\underline{k}} = -\phi_{\underline{k}} \, . \tag{20}$$

Thus, expressions of the form $\sum_{\vec{k}'} [\vec{k}_\perp \cdot (\vec{k}'_\perp \times \hat{n})]^2 \phi_{-\underline{k}'} \psi_{\underline{k}'}$ vanish identically. Substituting Eqs. (17) and (18) into Eqs. (6) and (7) while using Eqs. (19) and (20) yields the renormalized reduced resistive magnetohydrodynamic equations:

$$\frac{\partial}{\partial t} \psi_{\underline{k}} + N_{1\underline{k}} = -ik_\parallel \phi_{\underline{k}} - \eta k_\perp^2 \psi_{\underline{k}} + F_{\underline{k}}^M , \tag{21}$$

$$\frac{\partial}{\partial t}(k_\perp^2 \phi_{\underline{k}}) + \mu k_\perp^4 \phi_{\underline{k}} = -ik_\parallel k_\perp^2 \psi_{\underline{k}} + N_{2\underline{k}} + F_{\underline{k}}^K , \tag{22}$$

where the renormalized nonlinearities are given by

$$N_{1\underline{k}} = \sum_{\vec{k}'} [\vec{k} \cdot (\vec{k}' \times \hat{n})] L_{\underline{k}''} \left\{ \frac{|\phi_{\underline{k}'}|^2}{\gamma''_\eta} \psi_{\underline{k}} - \frac{(k_\perp'^2 - k_\perp^2)}{k_\perp''^2} \frac{|\psi_{\underline{k}'}|^2}{\gamma''_\mu} \psi_{\underline{k}} \right\} , \tag{23}$$

$$N_{2\underline{k}} = \sum_{\vec{k}'} [\vec{k} \cdot (\vec{k}' \times \hat{n})]^2 (k_\perp'^2 - k_\perp''^2) L_{\underline{k}''} \left\{ \frac{|\psi_{\underline{k}'}|^2}{\gamma''_\eta} \phi_{\underline{k}} + \frac{(k_\perp^2 - k_\perp'^2)}{k_\perp''^2} \frac{|\phi_{\underline{k}'}|^2}{\gamma''_\mu} \phi_{\underline{k}} \right\} . \tag{24}$$

The treatment of conservation laws and symmetries in the renormalized theory is now discussed. The nonlinear equations for Ψ and Φ conserve energy.[8] This property is easily demonstrated by multiplying Eq. (1) by J, and Eq. (2) by Φ, adding them, and then integrating over space. This yields the result

$$\frac{\partial}{\partial t}(E^M + E^K) + \eta \int d^3x J^2 + \mu \int d^3x U^2$$

$$= -\int d^3x (JF^M + \Phi F^K) , \tag{25}$$

where

$$E^M = \frac{1}{2} \int d^3x (\vec{\nabla}_\perp \Psi)^2 \tag{26}$$

and

$$E^K = \frac{1}{2} \int d^3x (\vec{\nabla}_\perp \Phi)^2 \tag{27}$$

are the magnetic and fluid kinetic energies, respectively. Equation (25) states that total energy is conserved up to the difference between drive by external forcing and dissipation by resistivity and viscosity. In deriving Eq. (25), the contributions to fluid-field energy exchange resulting from the $(\vec{\nabla}\Phi \times \hat{n}) \cdot \vec{\nabla}\Psi$ nonlinearity of Eq. (1) and the $(\vec{\nabla}\Psi \times \hat{n}) \cdot \vec{\nabla}J$ nonlinearity of Eq. (2) cancel, while the contribution from the convective nonlinearity, $(\vec{\nabla}\Phi \times \hat{n}) \cdot \vec{\nabla}U$, of Eq. (2) vanishes independently when integrated.

The energy conservation laws stated in Eq. (25) can be restated in the form $\Delta = 0$, where

$$\Delta = \int d^3x \{ J(\vec{\nabla}\Phi \times \hat{n}) \cdot \vec{\nabla}\Psi - \Phi(\vec{\nabla}\Psi \times \hat{n}) \cdot \vec{\nabla}J$$

$$+ \Phi(\vec{\nabla}\Phi \times \hat{n}) \cdot \vec{\nabla}U \} . \tag{28}$$

The closure scheme used to renormalize the reduced magnetohydrodynamic equations can now be applied to the calculation of Δ, yielding:

$$\Delta = \sum_{\vec{k}} \sum_{\vec{k}'} [\vec{k} \cdot (\vec{k}' \times \hat{n})] \{ J_{-\underline{k}} \phi_{-\underline{k}}, \psi^{(2)}_{\underline{k}+\underline{k}}, - J_{-\underline{k}} \psi_{-\underline{k}}, \phi^{(2)}_{\underline{k}+\underline{k}}, - J^{(2)}_{\underline{k}+\underline{k}}, \phi_{-\underline{k}}, \psi_{-\underline{k}} - \phi_{-\underline{k}} \psi_{-\underline{k}}, J^{(2)}_{\underline{k}+\underline{k}}, + \phi_{-\underline{k}} J_{-\underline{k}}, \psi^{(2)}_{\underline{k}+\underline{k}}, + J_{-\underline{k}} \psi_{-\underline{k}}, \phi^{(2)}_{\underline{k}+\underline{k}}, + \phi_{-\underline{k}} \phi_{-\underline{k}}, U^{(2)}_{\underline{k}+\underline{k}}, - \phi_{-\underline{k}} U_{-\underline{k}}, \phi^{(2)}_{\underline{k}+\underline{k}}, - \phi_{-\underline{k}}, U_{-\underline{k}} \phi^{(2)}_{\underline{k}+\underline{k}}, \} . \quad (29)$$

Here the driven quantities $\psi^{(2)}_{\underline{k}}$, $\phi^{(2)}_{\underline{k}}$, $J^{(2)}_{\underline{k}}$ and $U^{(2)}_{\underline{k}}$ are given by Eqs. (17) and (18). Upon exchanging $\vec{k}$ with $\vec{k}'$, the first, third, and eighth terms of the right-hand side of Eq. (29) cancel the fifth, fourth, and ninth, respectively, while the seventh vanishes identically. The second and sixth terms cancel directly. Thus $\Delta = 0$, and the closure scheme conserves energy. It should be noted that the $\psi^{(2)}_{\underline{k}}$, $J^{(2)}_{\underline{k}}$, and $\phi^{(2)}_{\underline{k}}$ contributions to $\int d^3x J(\vec{\nabla}\Phi \times \hat{n}) \cdot \vec{\nabla}\Psi$ cancel their counterparts in $\int d^3x \Phi(\vec{\nabla}\Psi \times \hat{n}) \cdot \vec{\nabla} J$, while the $\phi^{(2)}_{\underline{k}}$ contributions to $\int d^3x \phi(\vec{\nabla}\Phi \times \hat{n}) \cdot \vec{\nabla} U$ cancel and the $U^{(2)}_{\underline{k}}$ term vanishes independently. Hence, the renormalized theory maintains the separation between field-fluid energy exchange terms and the contribution from the purely fluid convective nonlinearity. Furthermore, it is clear that $\vec{k} \leftrightarrow \vec{k}'$ exchange symmetry of $\psi^{(2)}$ and $\phi^{(2)}$ and a consistent treatment of the Ohm's law and the equation of motion are sufficient conditions for $\Delta = 0$, while considerations of dynamics and geometry do not enter. However, because such considerations may have considerable impact on the results and physical predictions of the theory, it is worthwhile to insert the caveat that while it is clearly necessary for a given

closure scheme to conserve energy, it is also the case that such a property is not a particularly discerning diagnostic for renormalization schemes.

The third, sixth, and ninth terms in the expression for Δ are the result of contributions from incoherent emission effects, which appear in the renormalized spectrum (two-point) equations but not in the renormalized one-point equations considered here. Hence, contrary to the assertions of Ref. 15, it is meaningless to require conservation of energy in a one-point theory. Also, the fact that Eqs. (21) and (22) do not conserve energy does not diminish their utility for studying the effects of turbulence on tearing instabilities. We will discuss the renormalized spectrum equations, including incoherent emission effects, in a future publication.

In addition to energy, the behavior of the mean square poloidal flux is of considerable interest. Multiplying Eq. (1) by Ψ and integrating over space yields:

$$\frac{1}{2}\frac{\partial}{\partial t}\int d^3x\Psi^2 = -\int d^3x\Psi(\vec{\nabla}\Phi \times \hat{n}) \cdot \vec{\nabla}\Psi$$

$$-\eta \int d^3x\Psi J - \int d^3x\Psi \frac{\partial \Phi}{\partial z} + \int d^3x\Psi F^M$$

$$= \int d^3x\left\{-\eta\Psi J - \Psi \frac{\partial \Phi}{\partial z} + \Psi F^M\right\} . \qquad (30)$$

Thus, the nonlinearity $(\vec{\nabla}\Phi \times \hat{n}) \cdot \vec{\nabla}\Psi$ conserves mean square flux. In two dimensions, where $\partial\Phi/\partial z = 0$, mean square flux is conserved up to resistive dissipation and external forcing. For strongly turbulent, low $k_{\parallel}$ fluctuations in three dimensions, for which $|(\vec{\nabla}\Phi \times \hat{n}) \cdot \vec{\nabla}\Psi| > |\partial\Phi/\partial z|$, mean square flux can be regarded as an approximate invariant, apart from forcing and dissipation. Using the closure scheme to calculate the rate of change of mean square flux yields

$$\frac{\partial}{\partial t}\int d^3x\Psi^2 + \eta E^M + \int d^3x\left(\Psi\frac{\partial\Phi}{\partial z} - \Psi F^M\right)$$

$$= \sum_{\vec{k}}\sum_{\vec{k}'}\left[\vec{k}\cdot(\vec{k}'\times\hat{n})\right]\left\{\Psi_{-\underline{k}}\Phi_{-\underline{k}'}\Psi^{(2)}_{\underline{k}+\underline{k}'}\right.$$

$$\left. - \Psi_{-\underline{k}}\Psi_{-\underline{k}'}\Phi^{(2)}_{\underline{k}+\underline{k}'} - \Phi_{-\underline{k}'}\Psi_{-\underline{k}}\Psi^{(2)}_{\underline{k}+\underline{k}'}\right\} = 0 .$$

Thus, the closure scheme is consistent with the conservation of mean square flux by the nonlinearity of Eq. (1). Note that the coherent and incoherent driven flux terms cancel, while the $\Phi^{(2)}_{\underline{k}+\underline{k}'}$ term vanishes under interchange of $\vec{k}$ and $\vec{k}'$.

III. DISCUSSION OF THE RENORMALIZED REDUCED RESISTIVE MAGNETOHYDRODYNAMIC EQUATIONS

In this section, the renormalized reduced resistive magnetohydrodynamic equations are discussed in detail. Attention is focused on the physical origin, content, and interpretation of the effects appearing in the renormalized turbulence theory. The implications of the various effects for the dynamics of a tearing instability in a turbulent magneto-fluid is described.

The renormalized reduced resistive manetohydrodynamic equations are, from Eqs. (21) and (22),

$$\gamma_{\underline{k}}\psi_{\underline{k}} + ik_{\parallel}\phi_{\underline{k}} = \eta J_{\underline{k}} + d_{\underline{k}}\psi_{\underline{k}} + c_{\underline{k}}\psi_{\underline{k}} + F^{M}_{\underline{k}} \tag{31}$$

$$\gamma_{\underline{k}}(k_{\perp}^2\phi_{\underline{k}}) + \mu k_{\perp}^2(k_{\perp}^2\phi_{\underline{k}}) + \mu_{\underline{k}}\phi_{\underline{k}} = -ik_{\parallel}k_{\perp}^2\psi_{\underline{k}} + a_{\underline{k}}\phi_{\underline{k}} + F^{K}_{\underline{k}}\,, \tag{32}$$

where

$$d_{\underline{k}} = \sum_{\vec{k}'} \left[\vec{k}_{\perp} \cdot (\vec{k}'_{\perp} \times \hat{n})\right]^2 L_{\underline{k}''} \frac{|\phi_{\underline{k}'}|^2}{\gamma''_{\eta}}\,, \tag{33}$$

$$c_{\underline{k}} = \sum_{\vec{k}'} \left[\vec{k}_{\perp} \cdot (\vec{k}'_{\perp} \times \hat{n})\right]^2 L_{\underline{k}''} \left(\frac{k_{\perp}'^2 - k_{\perp}^2}{k_{\perp}''^2}\right) \frac{|\psi_{\underline{k}'}|^2}{\gamma''_{\mu}}\,, \tag{34}$$

$$\mu_{\underline{k}} = \sum_{\vec{k}'} \left[\vec{k}_{\perp} \cdot (\vec{k}'_{\perp} \times \hat{n})\right]^2 L_{\underline{k}''}(k_{\perp}'^2 - k_{\perp}''^2) \left(\frac{k_{\perp}'^2 - k_{\perp}^2}{k_{\perp}''^2}\right) \frac{|\phi_{\underline{k}'}|^2}{\gamma''_{\mu}}\,, \tag{35}$$

$$a_{\underline{k}} = \sum_{\vec{k}'} \left[\vec{k}_{\perp} \cdot (\vec{k}'_{\perp} \times \hat{n})\right]^2 L_{\underline{k}''}(k_{\perp}'^2 - k_{\perp}''^2) \frac{|\psi_{\underline{k}'}|^2}{\gamma''_{\eta}}\,. \tag{36}$$

Equation (31) is the renormalized Ohm's law. After implementation of closure, the $(\vec{\nabla}\Phi \times \hat{n}) \cdot \vec{\nabla}\Psi$ nonlinearity yields two classes of effects, represented by $d_{\underline{k}}$ and $c_{\underline{k}}$, respectively. The first effect, $d_{\underline{k}}$, arises from the interaction of background fluid turbulence with the nonlinearly driven flux $\psi_{\underline{k}}^{(2)}$. The $d_{\underline{k}}$ accounts for the process of random convection of magnetic flux by fluid turbulence and appears as an anomalous ohmic diffusivity (resistivity) that dissipates magnetic energy. Thus, the presence of short wavelength fluid turbulence can significantly enhance the effective dissipation acting on a long wavelength magnetic perturbation. Anticipating later application to reduced magnetohydrodynamic turbulence in a sheared magnetic field, $d_{\underline{k}}\psi_{\underline{k}}$ will appear as a diffusion of magnetic flux $(D_{\underline{k}}\, \partial^2 \psi_{\underline{k}}/\partial x^2)$, an effect that is especially significant near the $\vec{k} \cdot \vec{B}_0 = 0$ surface of a long wavelength tearing instability.

The second nonlinear effect in Eq. (31), $c_{\underline{k}}\psi_{\underline{k}}$, is derived from the interaction of magnetic turbulence with the nonlinearly driven velocity perturbation associated with $\phi_{\underline{k}}^{(2)}$, and accounts for the back-reaction of the nonlinear Lorentz force on the evolution of the poloidal flux. Noting that the $\phi_{\underline{k}}^{(2)}$ contribution to $N_{1\underline{k}}$ conserves mean square flux, it follows that $c_{\underline{k}}$ may be associated with the transfer or cascade of $\langle\psi^2\rangle$ from short to long wavelength. The association of $c_{\underline{k}}$ with a conservative transfer process, rather than with a purely dissipative mechanism, is consistent with the observation that, at long wavelengths where $|\vec{k}_\perp| < |\vec{k}'_\perp|$, one has

$$c_{\underline{k}} \cong \sum_{\vec{k}'} [\vec{k}_\perp \cdot (\vec{k}'_\perp \times \hat{n})]^2 L_{\underline{k}''} \frac{|\psi_{\underline{k}'}|^2}{\gamma''_\mu} , \qquad (37)$$

while at short wavelengths where $|\vec{k}| > |\vec{k}'|$,

$$c_{\underline{k}} \cong - \sum_{\vec{k}'} \left[\vec{k}_\perp \cdot (\vec{k}'_\perp \times \hat{n})\right]^2 L_{\underline{k}''} \frac{|\psi_{\underline{k}'}|^2}{\gamma_\mu} \quad . \tag{38}$$

Thus, the $\langle\psi^2\rangle$ cascade increases the population at larger scales while depleting it at smaller scales. This cascade reflects the natural tendency of a system of current and magnetic fluctuations to arrange itself (by driving fluid motion) so that flux accumulates at large scales, where the $\vec{B} \cdot \vec{\nabla} J_\parallel$ driving force is minimal. Hence, the $\langle\psi^2\rangle$ cascade resembles the phenomenon of magnetic island coalescence[18].

In a recent publication,[19] the $\langle\psi^2\rangle$ cascade has been associated with a negative anomalous resistivity. While Eq. (37) indicates that such an interpretation is valid for long wavelength fluctuations, it clearly omits the depletion of small-scale flux that accompanies the growth of and, in fact, feeds the large scale flux. Hence, the simple, negative anomalous resistivity misrepresents a basically conservative cascade process as a dissipation mechanism. Furthermore, in view of the $k''^{-2}_\perp$ factor in $c_{\underline{k}}$, representation of the cascade of $\langle\psi^2\rangle$ with local diffusion operators is highly dubious. In fact, a result in the next section, will show that, in the case of magnetohydrodynamic turbulence in a sheared magnetic field, there is no significant contribution equivalent to $c_{\underline{k}}$ in the renormalized equations.

Equation (32) is the renormalized equation of motion. The nonlinear effect $a_{\underline{k}}\phi_{\underline{k}}$ is derived from the interaction of magnetic turbulence with the nonlinearly driven flux and current perturbations $\psi_{\underline{k}''}^{(2)}$ and $J_{\underline{k}''}^{(2)}$, which contribute to the $k_{\perp}'^2$ and $k_{\perp}''^2$ terms respectively in $a_{\underline{k}}$. The $a_{\underline{k}}$ accounts for the stress exerted on the fluid by magnetic turbulence. This influence may be seen by noting that $k_{\perp}'^2 - k_{\perp}''^2 = -2\vec{k}_{\perp} \cdot \vec{k}_{\perp}' - k_{\perp}^2$ and that $\vec{k}_{\perp} \cdot \vec{k}_{\perp}'$ vanishes upon summation of $\vec{k}_{\perp}'$, yielding

$$a_{\underline{k}} \cong - k_{\perp}^2 \sum_{\vec{k}'} \left[\vec{k}_{\perp} \cdot (\vec{k}_{\perp}' \times \hat{n})\right]^2 L_{\underline{k}''} \frac{|\psi_{\underline{k}'}|^2}{\gamma_{\eta}''} . \tag{39}$$

Hence, in the context of the local analysis followed here, $a_{\underline{k}}$ damps vorticity and can be interpreted as an anomalous magnetic vorticity damping. This conclusion agrees with that of Ref. (19). Indeed, $a_{\underline{k}}$ is the reduced magnetohydrodynamics analogue of the Alfvén effect, first noted by Kraichnan.[20,21] The Alfvén effect refers to the phenomenon of damping of fluid motion by coupling, via the $\vec{B} \cdot \vec{\nabla} J$ torque, to magnetic perturbations and Alfvén waves. However, in the case of turbulence in a sheared magnetic field, it will be shown that $k_{\perp}''^2$ is replaced by $-\Delta_{\underline{k}''}' \delta(x'')$. Thus, considerations of geometry and energetics can change the apparent sign of effects associated with the interaction of field and fluid.

It is interesting to note that the $J_{\underset{\sim}{k}}^{(2)}$ contribution opposes vorticity growth, while the $\psi_{\underset{\sim}{k}}^{(2)}$ contribution drives fluid vorticity. The latter follows from the fact that energy conservation requires that $\psi_{\underset{\sim}{k}}^{(2)}$ induced effects in the equation of motion destabilize kinetic energy because the $\psi_{\underset{\sim}{k}}^{(2)}$ contribution to the renormalized Ohm's law ($d_{\underset{\sim}{k}}$) dissipates magnetic energy.

The second nonlinear effect $\mu_{\underset{\sim}{k}}$, in the equation of motion, results from the renormalization of the convective nonlinearity. As the physical processes that underlie $\mu_{\underset{\sim}{k}}$ have been thoroughly described in the literature of hydrodynamic turbulence,[22,23] this effect will not be discussed further here.

The results of this discussion may be summarized by writing the renormalized reduced resistive magnetohydrodynamic equations for a long wavelength ($|\vec{k}| < |\vec{k}'|$) fluctuation:

$$\gamma_{\underset{\sim}{k}}\psi_{\underset{\sim}{k}} + ik_{\parallel}\phi_{\underset{\sim}{k}} = -(d_{\underset{\sim}{k}} - c_{\underset{\sim}{k}}^{(0)})\psi_{\underset{\sim}{k}} - \eta k_{\perp}^2\psi_{\underset{\sim}{k}} + F_{\underset{\sim}{k}}^{M} \tag{40}$$

and

$$\gamma_{\underset{\sim}{k}}k_{\perp}^2\phi_{\underset{\sim}{k}} + (\mu k_{\perp}^2 + \mu_{\underset{\sim}{k}})\phi_{\underset{\sim}{k}} = -ik_{\parallel}k_{\perp}^2\psi_{\underset{\sim}{k}} + a_{\underset{\sim}{k}}\phi_{\underset{\sim}{k}} + F_{\underset{\sim}{k}}^{K} \tag{41}$$

where

$$d_{\underset{\sim}{k}} = \sum_{\vec{k}'} [\vec{k}_{\perp} \cdot (\vec{k}_{\perp}' \times \hat{n})]^2 \, L_{\underset{\sim}{k}''} \frac{|\phi_{\underset{\sim}{k}'}|^2}{\gamma_{\eta}''} , \tag{42}$$

$$c_{\underset{\sim}{k}}^{(0)} \cong \sum_{\vec{k}'} [\vec{k}_{\perp} \cdot (\vec{k}_{\perp}' \times \hat{n})]^2 \, L_{\underset{\sim}{k}''} \frac{|\psi_{\underset{\sim}{k}'}|^2}{\gamma_{\mu}''} , \tag{43}$$

$$a_{\underset{\sim}{k}} \cong -k_{\perp}^2 \sum_{\underset{\sim}{k}_{\perp}} [\vec{k}_{\perp} \cdot (\vec{k}_{\perp}' \times \hat{n})]^2 \, L_{\underset{\sim}{k}''} \frac{|\psi_{\underset{\sim}{k}'}|^2}{\gamma_{\eta}''} , \tag{44}$$

$$\mu_{\underline{k}} \cong k_\perp^2 \sum_{\vec{k}'} [\vec{k}_\perp \cdot (\vec{k}'_\perp \times \hat{n})]^2 \, L_{k''} \frac{|\phi_{\underline{k}'}|^2}{\gamma''_\mu} \quad . \tag{45}$$

When $d_{\underline{k}} \cong c_{\underline{k}}^{(0)}$, which loosely corresponds to the case of equipartition of energy between fluid and magnetic turbulence, it is necessary to retain the order $k_\perp^2/k_\perp'^2$ piece of $c_{\underline{k}}$, which is:

$$c_{\underline{k}}^{(1)} \cong -k_\perp^2 \sum_{\vec{k}'} \frac{[\vec{k}_\perp \cdot (\vec{k}'_\perp \times \hat{n})]^2}{k_\perp'^2} L_{k''} \frac{|\psi_{\underline{k}'}|^2}{\gamma''_\mu} \tag{46}$$

In that case, $c_{\underline{k}}^{(1)}$ constitutes a positive anomalous ohmic viscosity due to magnetic turbulence.

IV. RENORMALIZED EQUATIONS FOR MULTIPLE-HELICITY TURBULENCE IN A SHEARED MAGNETIC FIELD

In this section, the renormalized equations that describe the evolution of a long wavelength tearing instability in the presence of multiple-helicity turbulence in a sheared magnetic field are derived and discussed. The renormalization procedure described in the previous sections is used. However, the consideration of magnetic shear and the consequent differing spatial orientations of fluctuations and resonances of varying helicity result in renormalized equations of significantly different structure than Eqs. (40) and (41).

The reduced resistive magnetohydrodynamic equations for a current-carrying magneto-fluid in a sheared slab are:

$$\frac{\partial \psi_{\underline{k}}}{\partial t} + \left\{\left[\frac{\partial}{\partial r}\left(\sum_{\vec{k}'} (-ik_y')\phi_{-\underline{k}'}\psi_{\underline{k}''}\right) - ik_y \sum_{\vec{k}'} \frac{\partial \phi_{-\underline{k}'}}{\partial r}\psi_{\underline{k}''}\right]\right.$$
$$\left. - \left[\frac{\partial}{\partial r}\left(\sum_{\vec{k}'} (-ik_y')\psi_{-\underline{k}'}\phi_{\underline{k}''}\right) - ik_y \sum_{\vec{k}'} \frac{\partial \psi_{-\underline{k}'}}{\partial r}\phi_{\underline{k}''}\right]\right\}$$
$$= -ik_{\parallel}\phi_{\underline{k}} + \eta\vec{\nabla}_{\perp}^2\psi_{\underline{k}} \qquad (47)$$

and

$$\frac{\partial}{\partial t}(\vec{\nabla}_{\perp}^2\phi_{\underline{k}}) + \left\{\left[\frac{\partial}{\partial r}\left(\sum_{\vec{k}'} (-ik_y')\phi_{-\underline{k}'}\vec{\nabla}_{\perp}^2\phi_{\underline{k}''}\right) - ik_y \sum_{\vec{k}'} \frac{\partial \phi_{-\underline{k}'}}{\partial r}\vec{\nabla}_{\perp}^2\phi_{\underline{k}''}\right]\right.$$
$$\left. - \left[\frac{\partial}{\partial r}\left(\sum_{\vec{k}'} (-ik_y')(\vec{\nabla}_{\perp}^2\phi_{-\underline{k}'})\phi_{\underline{k}''}\right) - ik_y \sum_{\vec{k}'} \left(\frac{\partial}{\partial r}\vec{\nabla}_{\perp}^2\phi_{-\underline{k}'}\right)\phi_{\underline{k}''}\right]\right\}$$

$$= -ik_{\parallel}\vec{\nabla}_{\perp}^2\psi_{\underline{k}} + ik_y\frac{dJ_0(r)}{dr}\psi_{\underline{k}} + \left[\frac{\partial}{\partial r}\left(\sum_{\vec{k}'}(-ik_y')\psi_{-\underline{k}'}\vec{\nabla}_{\perp}^2\psi_{\underline{k}''}\right)\right.$$

$$- ik_y\sum_{\vec{k}'}\frac{\partial\psi_{-\underline{k}'}}{\partial r}\vec{\nabla}_{\perp}^2\psi_{\underline{k}''}\Bigg] - \left[\frac{\partial}{\partial r}\left(\sum_{\vec{k}'}(-ik_y')\vec{\nabla}_{\perp}^2\psi_{-\underline{k}'}\psi_{\underline{k}''}\right)\right.$$

$$\left.\left. - ik_y\sum_{\vec{k}'}\frac{\partial}{\partial r}(\vec{\nabla}_{\perp}^2\psi_{-\underline{k}'})\psi_{\underline{k}''}\right]\right\} . \qquad (48)$$

Here $\vec{k} = (k_y, k_z)$, where k_y and k_z are the wave numbers in the azimuthal and axial directions; and $\vec{\nabla}_{\perp}^2 \equiv \partial^2/\partial r^2 - k_y^2$, where r is the radial coordinate. The parallel wave number $k_{\parallel}$ is given by $k_{\parallel} = xk_y/L_s$, where the shear length L_s is defined by $L_s^{-1} = rq'/Rq^2$ and x is the distance from the singular surface where $\vec{k}\cdot\vec{B}_0 = 0$. For reasons of convenience, the collisional viscosity has been dropped. Note that the external forcing functions F^M and F^K are now unnecessary, since the current gradient, dJ_0/dr, exerts a torque that drives the fluid vorticity.

Equations (47) and (48) are renormalized by iteratively substituting the nonlinearly driven fields $\psi_{\underline{k}}^{(2)}$ and $\phi_{\underline{k}}^{(2)}$ for $\psi_{\underline{k}''}$ and $\phi_{\underline{k}''}$. The nonlinearly driven fields satisfy the equations

$$\frac{\partial\psi_{\underline{k}}^{(2)}}{\partial t} + ik_{\parallel}''\phi_{\underline{k}}^{(2)} - \eta J_{\underline{k}}^{(2)} = S_1 \qquad (49)$$

and

$$\frac{\partial}{\partial t}\vec{\nabla}_{\perp}^2\phi_{\underline{k}}^{(2)} + ik_{\parallel}''\vec{\nabla}_{\perp}^2\psi_{\underline{k}}^{(2)} - ik_y''\psi_{\underline{k}}^{(2)}\frac{dJ_0}{dr} = S_2 \ , \qquad (50)$$

where

$$S_1 = -\left[ik'_y \phi_{\underline{k}'} \frac{\partial \psi_{\underline{k}}}{\partial x} - \frac{\partial \phi_{\underline{k}'}}{\partial x} ik_y \psi_{\underline{k}} \right.$$

$$\left. + ik_y \phi_{\underline{k}} \frac{\partial \psi_{\underline{k}'}}{\partial x} - ik'_y \frac{\partial \phi_{\underline{k}}}{\partial x} \psi_{\underline{k}'} \right] , \qquad (51)$$

$$S_2 = \left[ik'_y \phi_{\underline{k}'} \frac{\partial}{\partial x} \left(\vec{\nabla}_\perp^2 \phi_{\underline{k}} \right) - ik_y \frac{\partial \phi_{\underline{k}'}}{\partial x} \vec{\nabla}_\perp^2 \phi_{\underline{k}} \right.$$

$$\left. + ik_y \phi_{\underline{k}} \frac{\partial}{\partial x} \left(\vec{\nabla}_\perp^2 \phi_{\underline{k}'} \right) - ik'_y \frac{\partial \phi_{\underline{k}}}{\partial x} \vec{\nabla}_\perp^2 \phi_{\underline{k}'} \right]$$

$$- \left[ik'_y \psi_{\underline{k}'} \frac{\partial}{\partial x} \left(\vec{\nabla}_\perp^2 \psi_{\underline{k}} \right) - ik_y \frac{\partial \psi_{\underline{k}'}}{\partial x} \vec{\nabla}_\perp^2 \psi_{\underline{k}} \right.$$

$$\left. + ik_y \psi_{\underline{k}} \frac{\partial}{\partial x} \left(\vec{\nabla}_\perp^2 \psi_{\underline{k}'} \right) - ik'_y \frac{\partial \psi_{\underline{k}}}{\partial x} \vec{\nabla}_\perp^2 \psi_{\underline{k}'} \right] . \qquad (52)$$

Here $k''_{\parallel} = k_{\parallel} + k'_{\parallel} = k''_y x''/L_s$, where x'' is the distance from the $\vec{k}'' \cdot \vec{B}_0 = 0$ singular surface. It is apparent that, because of the inclusion of magnetic shear, the relative spatial orientation of the test ($\vec{k}$), background ($\vec{k}'$), and driven ($\vec{k}''$) modes is a significant consideration in the solution of Eqs. (49) and (50) and the renormalization of Eqs. (47) and (48). In particular, while nonlinear effects are of greatest interest near the $\vec{k} \cdot \vec{B}_0 = 0$ surface of the test mode, the nonlinearly driven $\vec{k}''$ mode is, in effect, a driven magnetohydrodynamic kink-tearing mode, whose spatial structure varies with x''. Hence, the nonlinear effects induced at the $\vec{k} \cdot \vec{B}_0 = 0$ surface depend on the radial structure of the $\vec{k}''$ fluctuation, and therefore, on the separation of the $\vec{k} \cdot \vec{B}_0 = 0$ and $\vec{k}'' \cdot \vec{B}_0 = 0$ surfaces. Two cases can be defined. The first occurs when the

$\vec{k} \cdot \vec{B}_0 = 0$ surface falls in the exterior magnetohydrodynamic region of the driven $\vec{k}'' \cdot \vec{B}_0$ fluctuation. In this case, which corresponds to a turbulent system of a few, large-amplitude, overlapping kink-tearing modes, the $\vec{k}''$ fluctuation obeys a driven Newcomb equation. In the second case, which corresponds to fully developed, multiple-helicity turbulence, the $\vec{k} \cdot \vec{B}_0 = 0$ surface falls in or near the small $k_{\parallel}''$ inertial interior region of the driven fluctuation. This case is governed by Eqs. (49) and (50). The two cases are hereafter referred to as the cases of sparsely packed and densely packed turbulence, respectively. In both cases, and in contrast to the linear stability problem, the driven $\vec{k}''$ fluctuation equations are well behaved as $x'' \to 0$, for $\eta = 0$. This absence of singular behavior is due to the driving by nonlinear interaction with growing modes on neighboring rational surfaces. Furthermore, in the case of sparsely and densely packed turbulence, $\gamma_{\underline{k}}$ and $\gamma_{\underline{k}} + \gamma_{\underline{k}'}$, respectively, are anomalously large and independent of collisional resistivity. Therefore, the collisional resistivity is neglected in the following discussion of the solution of Eqs. (49) and (50). In addition, the anomalously large growth rates and the ordering $k_x' x_a'' < 1$ (which indicates that near $x \simeq 0$, x'' is finite) eliminate the need to consider renormalization effects in calculating the driven fields. Here x_a'' is the inertial layer width of the nonlinearly driven fluctuation.

In the case of sparsely packed turbulence,[10] the $\vec{k} \cdot \vec{B}_0 = 0$ surface falls in the exterior, Newcomb region of the $\vec{k}''$ fluctuation. The driven flux $\psi_{\underline{k}}^{(2)}$ obeys an inhomogeneous Newcomb equation, where the source is the current of the $\vec{k}''$ fluctuation, which appears as a localized discontinuity in $\partial\psi_{\underline{k}''}/\partial r$ at $x'' = 0$. Therefore, $\psi_{\underline{k}''}^{(2)}$ and $\phi_{\underline{k}''}^{(2)}$ satisfy the equations

$$\vec{\nabla}_\perp^2 \psi_{\underline{k}''}^{(2)} - \frac{L_s}{x''}\frac{dJ_0}{dr}\psi_{\underline{k}''}^{(2)} = \psi_{\underline{k}''}^{(2)}(0)\Delta'_{\underline{k}''}\,\delta(x'') \tag{53}$$

and

$$\gamma_{\underline{k}''}\psi_{\underline{k}''}^{(2)} + ik_\parallel''\phi_{\underline{k}''}^{(2)} = S_1^{\sim} \quad . \tag{54}$$

Here $\psi_{\underline{k}''}^{(2)}(0)$ is the value of $\psi_{\underline{k}''}^{(2)}$ at $x'' = 0$, $\Delta'_{\underline{k}''}$ is the discontinuity in $\partial\psi_{\underline{k}''}^{(2)}/\partial r$ induced by the current sheet localized at $x'' = 0$, and $\delta(x)$ is the Dirac delta function. It follows straightforwardly that

$$\psi_{\underline{k}''}^{(2)} = \psi_{\underline{k}''}^{(2)}(0)\Delta'_{\underline{k}''}\,G_N(x'',0) \quad , \tag{55}$$

$$J_{\underline{k}''}^{(2)} = \psi_{\underline{k}''}^{(2)}(0)\,\Delta'_{\underline{k}''}\,\delta(x'') \quad , \tag{56}$$

and

$$\phi_{\underline{k}''}^{(2)} = \frac{i}{k_\parallel''}\left(\gamma''\psi_{\underline{k}''}^{(2)}(0)\Delta'_{\underline{k}''}G_N(x'',0) - S_1\right) \quad , \tag{57}$$

where

$$\psi_{\underline{k}''}^{(2)}(0) = S_1/\gamma'' \quad . \tag{58}$$

Here, $G_N(x,x')$ is the Green's function for the Newcomb equation operator, $\vec{\nabla}_\perp^2 - (L_s/x)(dJ_0/dr)$. The driven vorticity, $\nabla_\perp^2\phi_{\underline{k}''}^{(2)}$, is

negligible, and, because $k_{\parallel}''$ is large, the driven potential $\phi_{\underset{\sim}{k}}^{(2)}$ is small. Substituting the nonlinearly driven fields into Eqs. (47) and (48), recalling that $\psi_{-\underline{k}} = \psi_{\underline{k}}$ and $\phi_{-\underline{k}} = -\phi_{\underline{k}}$, and assuming the tearing mode ordering $k_x >> k_y$ for the mode $\vec{k}$ gives

$$\gamma_{\underline{k}}\psi_{\underline{k}} + ik_{\parallel}\phi_{\underline{k}} = (\eta + D_{\underline{k}}) \frac{\partial^2\psi_{\underline{k}}}{\partial x^2} \tag{59}$$

and

$$\gamma_{\underline{k}} \frac{\partial^2\phi_{\underline{k}}}{\partial x^2} + ik_{\parallel} \frac{\partial^2\psi_{\underline{k}}}{\partial x^2} = a_{\underline{k}} \frac{\partial^2\phi_{\underline{k}}}{\partial x^2} \quad , \tag{60}$$

with

$$D_{\underline{k}} = \sum_{\vec{k}'} k_y'^2 \Delta_{\underline{k}'}' G_N(x'',0) \frac{|\phi_{\underline{k}'}|^2}{\gamma''} \quad , \tag{61}$$

$$a_{\underline{k}} = \sum_{\vec{k}'} \frac{k_y'^2}{\gamma''} \Delta_{\underline{k}'}' \left[|\psi_{\underline{k}'}|^2 \delta(x'') - |J_{\underline{k}'}\psi_{\underline{k}'}| \, G_N(x'',0) \right] \quad . \tag{62}$$

Here, $D_{\underline{k}}$ is an anomalous ohmic diffusivity, while $a_{\underline{k}}$ accounts for the stress of magnetic turbulence on the fluid motion. Note that $a_{\underline{k}}$ does not have the form of an eddy viscosity and can in fact be positive, thus destabilizing vorticity. This is plausible because positive $a_{\underline{k}}$ requires $\Delta_{\underline{k}'}' > 0$, thereby coupling the fluid to unstable magnetic perturbations.

In Ref. 10, this description of sparsely packed magnetohydrodynamic turbulence was applied to the rapid destabilization of the (m=3;n=2) tearing mode after the overlap of the 2/1 and 3/2 magnetic islands. In that case, the (m=2;n=1) mode is large and stationary and has a broad current perturbation. Thus, treating the (m=2;n=1) mode as the background $\vec{k}'$ fluctuation with $\gamma_{\underline{k}'} = 0$, it follows that $D_{\underline{k}}$ is negligible and that

$$a_{\underline{k}} \cong \sum_{\vec{k}'} \frac{k_y'^2}{\gamma_{\underline{k}}} \Delta'_{\underline{k}''} |\psi_{\underline{k}'}|^2 \delta(x'') \quad . \tag{63}$$

Equation (63) follows from the fact that $k_y > k'_y$ here, which is contrary to the usual scenario used in turbulence problems. The Δ' value for the driven (m=5;n=3) mode can be large and positive because of dJ_0/dr steepens at the $q = 5/3$ region when the 2/1 and 3/2 islands approach overlap. Hence, the nonlinear interaction of the driven (m=5;n=3) mode (with Δ' large and positive) with the (m=2;n=1) mode produces a magnetic stress on the fluid that destabilizes the kinetic energy of the (m=3;n=2) mode. Because of this rapid nonlinear destabilization, the (m=3;n=2) mode grows at the rate

$$\gamma_{\underline{k}} = \left(\sum_{\vec{k}'} k_y'^2 \Delta'_{\underline{k}''} \delta(x'') |\psi_{\underline{k}'}|^2 \right)^{1/2} \quad . \tag{64}$$

The nonlinear coupling process generates a localized fluid vortex near the $\vec{k} \cdot \vec{B} = 0$ surface of the (m=3;n=2) mode.

The flow of energy in the (m=3;n=2) mode destabilization process is easily traced. Initially, the current gradient steepens as it is pinched between the 3/2 and 2/1 islands. The (m=5;n=3) tearing mode is destabilized by a basically linear tearing process. The nonlinear interaction of the (m=5;n=3) mode and the stationary (m=2;n=1) mode then extracts magnetic energy from the (m=5;n=3) mode and destabilizes the kinetic energy of the (m=3;n=2) mode. It is important to emphasize that there are two different mechanisms operating: (1) the linear destabilization of the (m=5;n=3) and (2) the nonlinear coupling that drives the kinetic energy of the (m=3;n=2).

The more interesting case of densely packed, fully developed turbulence is now discussed. In this case, the driven, coupled magnetohydrodynamic equations must be solved for $\psi_{\underset{\sim}{k}}^{(2)}$ and $\phi_{\underset{\sim}{k}}^{(2)}$. These equations can be written in a simplified form:

$$\psi + iKx\phi = B_1 \tag{65}$$

and

$$\frac{\partial^2\phi}{\partial x^2} + iKx\,\frac{\partial^2\psi}{\partial x^2} = B_2 \,. \tag{66}$$

Here, x refers to x'' (the distance from the $\vec{k}'' \cdot \vec{B}_0 = 0$ surface), $\psi \equiv \psi_{\underset{\sim}{k}}^{(2)}$, $\phi \equiv \phi_{\underset{\sim}{k}}^{(2)}$, $B_1 = S_1/\gamma''$, $B_2 = S_2/\gamma''$, $\gamma'' \equiv \gamma_{\underset{\sim}{k}''}$, and $K = k_y''/(L_s\gamma'') = 1/x_a''$ (where x_a'' is the inertial layer width of the nonlinearly driven fluctuation). In addition, the tearing ordering $k_x^2 > k_y^2$ is adopted. Because the nonlinear evolution of a long wavelength tearing instability in the presence of a short wavelength turbulence is the phenomenon to be studied, $k_y' > k_y$ is assumed

throughout. It is also assumed that the radial widths of the spectra of background turbulence are equal to or exceed x_a'' ($k_x' x_a'' < 1$), rendering x_a'' the smallest radial scale in the system. Finally, it should be mentioned that although this calculation does not self-consistently treat the evolution of the background turbulence, the interaction of the background and the test mode is treated consistently, within the framework of reduced magnetohydrodynamics.

A solution of Eqs. (65) and (66) can be constructed by integrating Eq. (66) to obtain $\partial\phi/\partial x$, and then equating that expression to the result of differentiating Eq. (65), yielding:

$$N_2 - iKx^2 \frac{\partial}{\partial x}\left(\frac{\psi}{x}\right) + C = \frac{-i}{K}\left[\frac{\partial}{\partial x}\left(\frac{B_1}{x}\right) - \frac{\partial}{\partial x}\left(\frac{\psi}{x}\right)\right] \tag{67}$$

with

$$N_2 = \int B_2 \, dx \tag{68}$$

and C the constant of integration. Eq. (67) can be rewritten in the form

$$x^2 \frac{\partial}{\partial x}\left(\frac{\psi}{x}\right) = \frac{x^2}{1 + K^2x^2}\left[\frac{\partial}{\partial x}\left(\frac{B_1}{x}\right) - iKN_2 - iKC\right] . \tag{69}$$

Noting that

$$J_{\underline{k}}^{(2)} = \frac{1}{x}\frac{\partial}{\partial x}\left[x^2 \frac{\partial}{\partial x}\left(\frac{\psi}{x}\right)\right] , \tag{70}$$

it follows directly that the nonlinearly driven current $J_{\underline{k}}^{(2)}$ is given by

$$J_{\underset{\sim}{k}}^{(2)} = \frac{2}{(1 + K^2x^2)^2}\left(K^2B_1 - iKC - iKN_2\right) - \frac{iKxB_2}{1 + K^2x^2} \quad , \tag{71}$$

where B_1 is assumed to be approximately constant in x.

The factor $(1 + K^2x^2)^{-1}$, which is analogous to the resonance operator $L_{\underset{\sim}{k}''}$ of Sec. II, shows that driven fluctuations are heavily damped by magnetic field line bending and indicates that the driven current is localized around the $\vec{k}'' \cdot \vec{B}_0 = 0$ resonant surface of the beat mode.

The integration constant C is determined by imposing the boundary condition that ψ match the driven, exterior Newcomb solution as x'' becomes large. This requires that for $\partial^2\psi/\partial x^2 = J_{\underset{\sim}{k}}^{(2)}$,

$$\Delta'\psi_0 = \int_{-\infty}^{\infty} dx\, J_{\underset{\sim}{k}}^{(2)} \quad , \tag{72}$$

where ψ_0 is defined by the condition that for large x, $\psi \to \psi_0 + \psi_{\pm}'x$, with $\Delta' = (\psi_+' - \psi_-')/\psi_0$. In the problem discussed here, it will ultimately be shown that $\psi_0 = \psi(0)$. The accompanying condition that ψ be an even function of x determines a second integration constant that appears later in the calculation. By imposition of these boundary conditions, it is tacitly assumed that the driven $\vec{k}''$ fluctuations have the basic structure of kink-tearing modes. This observation seems consistent with the presence of shear and $\vec{k} \cdot \vec{B}_0 = 0$ resonances. Using Eq. (72), C is determined by

$$C = i\Delta'\psi_0/\pi - iKB_1 - N_2 \tag{73}$$

and

$$J_{\underline{k}}^{(2)} = \frac{2K\Delta'\psi_0/\pi}{(1 + K^2x^2)^2} - \frac{iKxB_2}{1 + K^2x^2} \quad . \tag{74}$$

Substituting $J_{\underline{k}}^{(2)}$ into Eq. (66) determines the driven vorticity:

$$\frac{\partial^2\phi}{\partial x^2} = \frac{K^2B_2x^2}{1 + K^2x^2} - \frac{2iK^2x(\Delta'\psi_0/\pi)}{(1 + K^2x^2)^2} \quad . \tag{75}$$

The driven flux and potential ψ and ϕ are determined from Eqs. (69), (70), and (74). Integration of Eq. (69) using the result of Eq. (73) gives:

$$\frac{\psi}{x} = \frac{B_1}{x} + \frac{\Delta'\psi_o}{\pi}\left(\tan^{-1}Kx + \frac{\pi}{2}\right) + C' \quad . \tag{76}$$

The condition that ψ be an even function of x determines the constant C'. It then follows that

$$C' = -\frac{\Delta'\psi_o}{2} \tag{77}$$

and

$$\psi = B_1 + \frac{\Delta'\psi_o}{\pi}\, x\tan^{-1}Kx \quad . \tag{78}$$

The value of ψ_o can now be determined by using Eq. (76), which states that

$$\frac{\partial}{\partial x}\left(\frac{\psi}{x}\right) \simeq -\frac{B_1}{x^2} + \frac{K\Delta'\psi_o/\pi}{1 + K^2x^2} \quad , \tag{79}$$

and by recalling the definition of ψ_o. Straightforward algebra yields:

$$\psi_o = B_1/(1 + x_a''\Delta'/\pi) \simeq B_1 \tag{80}$$

for $|x_a'' \Delta'| \ll 1$. Finally, substituting of ψ into Eq. (65) determines ϕ, where

$$\phi = ix_a'' \frac{\Delta'\psi_o}{\pi} \tan^{-1}(Kx) \quad . \tag{81}$$

The results of the calculation of the nonlinearly driven field may be summarized as:

$$\psi_{\underline{k}''}^{(2)} = \frac{S_1}{\gamma''}\left[1 + \Delta'_{\underline{k}''} \frac{x''}{\pi} \tan^{-1}\left(\frac{x''}{x_a''}\right)\right] \quad , \tag{82}$$

$$J_{\underline{k}''}^{(2)} = \frac{S_1}{\gamma''} \frac{2\Delta'_{\underline{k}''}}{\pi} \frac{(x_a'')^{-1}}{(1 + x''^2/x_a''^2)^2} \quad , \tag{83}$$

$$\frac{\partial^2 \phi_{\underline{k}''}^{(2)}}{\partial x^2} = \frac{S_2}{\gamma''} \frac{1}{1 + x''^2/x_a''^2} \quad , \tag{84}$$

and

$$\phi_{\underline{k}''}^{(2)} \approx 0 \quad . \tag{85}$$

Terms that do not contribute nonlinear effects to, and that break the tearing parity of the test mode equation have been dropped. The smooth transition between the results of Eqs. (82) — (85) and the driven exterior solutions given in Eqs. (55) — (58) can be illustrated by noting the limit of small x_a'':

$$J_{\underset{\sim}{k}}^{(2)} = \frac{S_1}{\gamma''}\frac{2\Delta'_{\underset{\sim}{k}''}}{\pi}\frac{(x_a'')^3}{(x''^2 + x_a''^2)^2} \cong \frac{S_1}{\gamma''}\Delta'_{\underset{\sim}{k}''}\delta(x'') \tag{86}$$

and

$$\psi_{\underset{\sim}{k}}^{(2)} = \frac{S_1}{\gamma''}\left[1 + \Delta'_{\underset{\sim}{k}''}G_N(x'')\right] , \tag{87}$$

where

$$-G_N(x'') = \frac{x''}{\pi}\tan^{-1}\left(\frac{x''}{x_a''}\right) \cong \begin{cases} \dfrac{x''}{2} & x'' > 0 \\ -\dfrac{x''}{2} & x'' < 0 \end{cases} . \tag{88}$$

Verification that $\partial^2 G_N(x'',0)/\partial^2 x'' = \delta(x'')$ is straightforward. Hence, for $x'' > x_a''$, $J_{\underset{\sim}{k}}^{(2)}$ smoothly matches to the driven exterior solutions. Also, consistent with the picture of the driven kink-tearing mode, the driven vorticity is localized to within the inertial layer ($|x| < x_a''$) around the $\vec{k}'' \cdot \vec{B}_o$ resonance point, while the driven potential $\phi_{\underset{\sim}{k}}^{(2)}$

varies rapidly across it. Furthermore, the localization of the driven vorticity to the narrow inertial layer implies that the nonlinearity of the equation of motion makes a negligible contribution to $\phi_{\underline{k}}^{(2)}$. Thus, it is apparent that magnetic shear has significant impact on the structure of the driven fluctuations and on the renormalized equations.

The renormalized reduced magnetohydrodynamic equations are now constructed by substituting Eqs. (82) — (85) into Eqs. (47) and (48), recalling the symmetry relation in Eqs. (19) and (20) and requiring that the tearing parity of the test mode equation be maintained. The tearing ordering $k_x > k_y$ is assumed. Thus, the renormalized equations are:

$$\gamma_{\underline{k}}\psi_{\underline{k}} + ik_{\parallel}\phi_{\underline{k}} - D_{\underline{k}}^{A}\frac{\partial^2\psi_{\underline{k}}}{\partial x^2} = \eta J_{\underline{k}} \tag{89}$$

and

$$\gamma_{\underline{k}}\frac{\partial^2\phi_{\underline{k}}}{\partial x^2} + \mu_{\underline{k}}\frac{\partial^2\phi_{\underline{k}}}{\partial x^2} + ik_{\parallel}\frac{\partial^2\psi_{\underline{k}}}{\partial x^2} = a_{\underline{k}}\frac{\partial^2\phi_{\underline{k}}}{\partial x^2} \quad , \tag{90}$$

where

$$D_{\underline{k}}^{A} = \sum_{\vec{k}'} k_y'^2 \frac{|\phi_{\underline{k}'}|^2}{\gamma''}\left[1 + \Delta_{\underline{k}'}'' G_N(x'')\right] \quad , \tag{91}$$

$$a_{\underline{k}} = \sum_{\vec{k}'} \frac{k_y'^2}{\gamma''}\left\{\Delta_{\underline{k}'}''|\psi_{\underline{k}'}|^2\delta(x'') - \left[1 + \Delta_{\underline{k}'}''G_N(x'')\right]|J_{\underline{k}'}\psi_{\underline{k}'}|\right\} \quad , \tag{92}$$

$$\mu_{\underline{k}} \frac{\partial^2 \phi_{\underline{k}}}{\partial x^2} = \sum_{\vec{k}'} \frac{k_y'^2}{\gamma''} \frac{1}{1 + \frac{x''}{x_a''}} \left(|\phi_{\underline{k}'}|^2 \frac{\partial^4 \phi_{\underline{k}}}{\partial x^4} - |\phi_{-\underline{k}'} \frac{\partial^2 \phi_{\underline{k}'}}{\partial x^2}| \frac{\partial^2 \phi_{\underline{k}}}{\partial x^2} \right) \quad . (93)$$

Note that $\phi_{\underline{k}}^{(2)}$ does not contribute any nonlinear effects to the test mode equations [Eqs. (89) and (90)]. Hence, in Eq. (89) no term is equivalent to the $c_{\underline{k}}$ contribution in the renormalized Eq. (31) derived from local theory. Equations (89) through (93) can be simplified by noting that the ordering $k_x' x_a'' < 1$ implies that effects derived from $\partial^2 \phi_{\underline{k}}^{(2)} / \partial x^2$ are of order $k_x' x_a'' < 1$. The localization of $\partial^2 \phi_{\underline{k}}^{(2)} / \partial x^2$ to the inertial layer around $\vec{k}'' \cdot \vec{B}_o = 0$ results in a reduction of the fluid viscosity. Hence, $\mu_{\underline{k}}$ is negligible in Eq. (90).

It should be mentioned that the principal results of this paper do not sensitively depend on detailed properties of the viscosity, because $\mu_{\underline{k}}$ is basically a fluid viscosity that has little effect on tearing modes for $\mu_{\underline{k}} \leq D_{\underline{k}}^A$.

Equations (89) through (93) can be simplified further by noting that terms of the form $\Delta_{\underline{k}'}'' G_N(x'', 0)$ are of order $\Delta_{\underline{k}'}'' / k_x'$ in comparison to unity. Since $|\Delta_{\underline{k}'}''| \leq |k_y'|$, and consistent with the tearing mode ordering $k_x' > k_y'$, it follows that $|\Delta_{\underline{k}'}'' / k_x'| < 1$. Therefore,

$$D_{\underline{k}}^A \cong \sum_{\vec{k}'} \frac{k_y'^2}{\gamma''} |\phi_{\underline{k}'}|^2 \quad . \tag{94}$$

Equation (92) can be simplified by noting that from Eq. (48)

$$a_{\underline{k}} \frac{\partial^2 \phi_{\underline{k}}}{\partial x^2} = \sum_{\vec{k}'} - i k_y' \left(\psi_{-\underline{k}'} \frac{\partial}{\partial x} \left(J_{\underline{k}+\underline{k}'}^{(2)} \right) - J_{-\underline{k}'} \frac{\partial}{\partial x} \left(\psi_{\underline{k}+\underline{k}'}^{(2)} \right) \right) . \tag{95}$$

In the case of densely packed turbulence, the summation over $\underline{k}'$ can be rewritten in the form $\int dm'dn'$. Changing variables from m' and n' to m' and x' and using $n' = m'/q$ yields:

$$\sum_{\vec{k}'} = \int dm' |m'| \frac{|q'|}{q^2} \int dx' \quad . \tag{96}$$

Hence, integrating the second term on the right-hand side of Eq. (95) twice by parts, noting that $d/dx' = (m'/m'')d/dx''$, yields:

$$a_{\underline{k}} \cong \sum_{\vec{k}'} \frac{k_y'^2}{\gamma''} \Delta_{\underline{k}'}'' \delta(x'') \frac{m^2}{m''^2} |\psi_{\underline{k}'}|^2 \quad . \tag{97}$$

In deriving Eq. (97), contributions added in m' were dropped; thus, the renormalized reduced magnetohydrodynamic equations for a long wavelength tearing mode instability in the presence of fully developed, densely packed turbulence are:

$$\gamma_{\underline{k}} \psi_{\underline{k}} + ik_{\parallel} \phi_{\underline{k}} = \left(D_{\underline{k}}^A + \eta\right) \frac{\partial^2 \psi_{\underline{k}}}{\partial x^2} \quad . \tag{98}$$

$$\gamma_{\underline{k}} \frac{\partial^2 \phi_{\underline{k}}}{\partial x^2} + ik_{\parallel} \frac{\partial^2 \psi_{\underline{k}}}{\partial x^2} = a_{\underline{k}} \frac{\partial^2 \phi_{\underline{k}}}{\partial x^2} \quad , \tag{99}$$

$$D_{\underline{k}}^A = \sum_{\vec{k}'} \frac{k_y'^2}{\gamma''} |\phi_{k'}|^2 \quad , \tag{100}$$

and

$$a_{\underline{k}} = \sum_{\underline{k}'} \frac{\Delta_{\underline{k}''}\delta(x'')}{\gamma''} \frac{m^2}{m''^2} k_y''^2 |\psi_{\underline{k}'}|^2 \quad . \tag{101}$$

Here, $D^A_{\underline{k}}$ is an anomalous ohmic diffusivity due to fluid convection of magnetic flux. The dependence of $D^A_{\underline{k}}$ on $(\gamma'')^{-1}$ indicates that the flux diffusion process is nonresonant in character. $a_{\underline{k}}$ is a stabilizing Alfvén effect due to the stress that magnetic turbulence exerts on the fluid vorticity. Note that $D^A_{\underline{k}}$ dissipates magnetic energy, while $a_{\underline{k}}$ damps fluid kinetic energy; hence, the anomalous dissipation in the Ohm's law is due to fluid turbulence, while the anomalous dissipation in the equation of motion is due to magnetic turbulence. This result disagrees with the conclusions of Ref. 16, in which an identical anomalous resistivity and viscosity appear in the renormalized equations.

V. ANOMALOUS TEARING INSTABILITY GROWTH AND DYNAMICS OF THE MAJOR DISRUPTION

In this section, the renormalized magnetohydrodynamic equations are solved, and the anomalous tearing instability growth rate is calculated. Also, the energetics of the accelerated growth process are described, and the dynamics of the major disruption in tokamaks are discussed. Specifically, the relation between the time scale of the negative voltage spike and the rate of anomalous tearing mode growth is determined.

To determine the anomalous tearing instability growth rate, the renormalized magnetohydrodynamic equations can be solved in the standard fashion.[3]

Because the case of interest is one characterized by high levels of fluid turbulence, $D_{\underline{k}}^{A} >> \eta$, the collisional resistivity is neglected hereafter. Equations (98) and (99) admit two classes of solution. The first class corresponds to a tearing instability triggered by the anomalous ohmic diffusivity $D_{\underline{k}}^{A}$, with the dispersion relation

$$\gamma_{\underline{k}}^{5} = \left(\frac{\sqrt{2}}{3}\right)^{4} \left(\Delta_{\underline{k}}'\right)^{4} \left(D_{\underline{k}}^{A}\right)^{3} \left(\frac{k_y}{L_s}\right)^{2} . \tag{102}$$

Because $D_{\underline{k}}^{A} \simeq (\gamma'')^{-1}$ and $\gamma'' \simeq \gamma_{\underline{k}}$, the anomalous tearing mode growth rate is

$$\gamma_{\underline{k}} = \left(\frac{\sqrt{2}}{3} \Delta_{\underline{k}}'\right)^{1/2} \left(\hat{D}\right)^{3/8} \left(\frac{k_y}{L_s}\right)^{1/4} , \tag{103}$$

where

$$\hat{D} = \sum_{\vec{k}} k_y'^2 \, |\phi_{\underline{k}'}|^2 \ . \tag{104}$$

The turbulently broadened tearing layer width is

$$\lambda_{\underline{k}} = \left(L_s/k_y\right)^{1/2} \hat{D}^{1/4} \ , \tag{105}$$

where $\gamma_{\underline{k}} > a_{\underline{k}}$ is required for consistency with the neglect of $a_{\underline{k}}$ in the calculation of the growth rate. Note that while the anomalous ohmic diffusivity accelerates the tearing mode growth, $\Delta'_{\underline{k}} > 0$ is still required for instability. The mode directly taps and releases magnetic free energy, thereby increasing fluctuation energy. Hence, the basic character of the instability is that of a linear tearing instability, substantially modified by nonlinear effects.

In contrast, the second class of solution corresponds to a localized fluid vortex ($\psi_{\underline{k}} = 0$) with growth rate

$$\gamma_{\underline{k}} = a_{\underline{k}} \ . \tag{106}$$

For $\Delta'_{\underline{k}} < 0$, the fluid vortex is damped. Hence, coupling of the damped vortex to the tearing process can result in a decrease in growth rate or termination of the tearing process. However, for $\gamma_{\underline{k}}^T > |a_{\underline{k}}|$, where $\gamma_{\underline{k}}^T$ is the nonlinear tearing growth rate given by Eq. (102), coupling to the damped fluid vortex has little or no effect. Because $\gamma_{\underline{k}}^T \sim \langle\phi^2\rangle^{3/8}$, while $|a_{\underline{k}}| \sim \langle\psi^2\rangle/\gamma_{\underline{k}}^T$ and $\langle\phi^2\rangle \sim \langle\psi^2\rangle$ at short wavelength, it follows that $|a_{\underline{k}}| \sim \langle\phi^2\rangle^{5/8}$ and thus $\gamma_{\underline{k}}^T > |a_{\underline{k}}|$. Hence $a_{\underline{k}}$ is hereafter neglected.

It is important to note that the rate at which magnetic free energy is actually released is anomalously large. This is in contrast to the model of Ref. 19, in which disruptive behavior is associated with the rapid transfer of magnetic energy from short to long wavelength. In that model, the mechanism for magnetic free energy release was not addressed. Finally, it is important to note that other nonlinear processes, such as incoherent mode coupling, may enter the dynamics of the short wavelength fluid turbulence.

One distinctive signature of the major disruption is a negative loop voltage spike associated with a change in the self-inductance of the plasma current.[4] The detailed behavior of the voltage trace during a tokamak disruption depends not only on the mechanism of the disruption process, but also on the external circuits of the tokamaks. Here we give a qualitative description of this phenomenon, using the simplest possible boundary conditions. We assume that the plasma current is constant in time. In this case, the change in voltage ΔV is given by:

$$\Delta V = \frac{1}{I}\frac{dE^M}{dt} \quad , \tag{107}$$

where I is the total current. Because the spectral distribution of evolving magnetic energy is dominated by the $\vec{k} = 0$ component, it is sufficient to consider this component only in the determination of ΔV. The $k = 0$ component of ψ, ψ_0, evolves according to:

$$\frac{\partial \psi_0}{\partial t} = -\frac{\partial}{\partial r}\left\langle \frac{\partial \phi}{\partial y}\psi \right\rangle + \eta J_0 \quad . \tag{108}$$

Equation (108) is derived by averaging Eq. (19) over y and z, where the averaging process is indicated by the angular brackets. Equation (108) states that the average poloidal flux evolves by radial convection and resistive dissipation. Here $\langle(\partial\phi/\partial y)\psi\rangle$ is the quasi-linear radial flux of magnetic flux. Multiplying Eq. (108) by J_0 and integrating over r gives:

$$\frac{dE_0^M}{dt} = -\int dr J_0 \frac{\partial}{\partial r}\left\langle\frac{\partial\phi}{\partial y}\psi\right\rangle , \tag{109}$$

where E_0^M is the $\vec{k} = 0$ component of magnetic energy and where the small amount of resistive dissipation is neglected. The correlation $\langle(\partial\phi/\partial y)\psi\rangle$ can be determined by multiplying the equation for ψ by $\partial\phi/\partial y$ and averaging:

$$\begin{aligned}\frac{\partial}{\partial t}\left\langle\frac{\partial\phi}{\partial y}\psi\right\rangle &= -\left\langle\left(\frac{\partial\phi}{\partial y}\right)^2\right\rangle\frac{\partial\psi_0}{\partial r} - \left\langle\frac{\partial\phi}{\partial y}\frac{\partial\phi}{\partial z}\right\rangle \\ &\cong -\left\langle\left(\frac{\partial\phi}{\partial y}\right)^2\right\rangle\frac{\partial\psi_0}{\partial r}\end{aligned} \tag{110}$$

for $k_z \ll k_y$. Mode coupling and resistivity have been neglected. It then follows straightforwardly that

$$\frac{dE_0^M}{dt} = -\int dr\, D^A J_0^2 \tag{111}$$

and

$$\Delta V = \frac{-1}{I}\int dr\, D^A J_0^2 \quad . \tag{112}$$

Thus, the plasma self-inductance changes through diffusive expulsion of poloidal flux due to turbulent fluid convection. Taken together, the relationships $D^A \sim 1/\gamma$ and $\gamma \sim (\hat{D})^{3/8}$ imply that $\Delta V \sim \hat{D}^{5/8}$. Therefore, the voltage spike mechanism and time scale are the same as the mechanism and time scale for the anomalous growth rate of the tearing mode.

VI. COMPARISON WITH NONLINEAR MULTIPLE-HELICITY NUMERICAL CALCULATIONS

To assess the consequences and validity of the theoretical model for major disruptions that has been developed in the previous sections, we have compared some of its predictions with the results of numerical calculations of multiple-helicity tearing mode interactions. For these calculations, the initial value code RSF[24] has been used. Details concerning this code and its numerical scheme can be found in Ref. 24. The numerical calculations are limited to cylindrical geometry, for consistency with the theoretical model. The calculations follow the nonlinear evolution of tearing modes, starting from an equilibrium that is linearly unstable to the (m=2;n=1) and (m=3;n=2) tearing modes. It is important to note that these calculations are not meant to be a detailed simulation of a tokamak disruption. The initial perturbations chosen are small enough to provide a separation in time of a sequence of phenomena that constitute the basic dynamic mechanisms involved in the nonlinear interaction of tearing modes. In this way, a sequence of phases in the calculation exists that can be studied on its own. In a realistic simulation of a disruption, some of these phases would be simultaneous. The main phases in the evolution are summarized in Fig. 1: initial numerical transient, linear phase, nonlinear Rutherford[9] regime, nonlinear interaction of 2/1 and 3/2 islands (sparsely packed turbulence), and development of high k turbulence. The first four phases of the calculation have been described in previous publications.[2,4] During these phases, radial grids with $\Delta r \simeq 10^{-2}$ and with up to 30 appropriately chosen modes generally give well-converged results.[24] The nonlinear interaction of the 2/1 and 3/2

modes through the 5/3 mode has been satisfactorily compared with the predictions of the sparsely packed turbulence model.[10] A description of the last phase will be given in this section, together with comparison to the predictions of the densely packed turbulence model given in Sec. V.

In the last phase of the calculation, when there is an approximate equipartition of energy among the high m modes, the growth rates of many modes are larger than the linear (m=2;n=1) tearing mode growth rate. At this point in the evolution, they become independent of the collisional resistivity η. This has been tested by raising or lowering the collisional resistivity at a certain time in the calculation. The results of these tests are summarized in Fig. 2, where the time evolution of the 3/2 magnetic island width has been plotted from $t = 2 \times 10^{-3}\tau_R$ up to the end of the calculation (broken line). The figure also shows the island width evolution after raising or lowering η by a factor of 3 at the following times: $2.06 \times 10^{-3}\tau_R$, $2.17 \times 10^{-3}\tau_R$, $2.22 \times 10^{-3}\tau_R$, $2.27 \times 10^{-3}\tau_R$, and $2.27 \times 10^{-3}\tau_R$. The increase (or decrease) in resistivity accelerates (or decelerates) the island width evolution except at the latest time, when it remains unaffected. The growth rates of the low m modes become independent of η for $t \geq 2.27 \times 10^{-3}\tau_R$. This result supports the analytic prediction that the dominant nonlinear effect in this process is an anomalous flux diffusivity due to turbulent fluid convection in the Ohm's law. This can be tested further by calculating the predicted growth rate [Eq. (103)] for the low m modes. The Δ' of the (m=3;n=2) mode is first calculated by numerically evaluating the linear growth rate of this mode at different times in the calculation. At these same times, $\hat{D}$

[given by Eq. (104)] is calculated from the numerical $\phi_{\underline{k}}$ spectrum. Then, using Eq. (103), the anomalous growth rate of the (m=3;n=2) mode is calculated, and its value can be compared with the nonlinear growth rate of this mode (Fig. 3). The agreement is good. It is also important to investigate the correlation of this anomalous growth with the buildup of the high m fluid turbulence under various circumstances. To investigate this buildup, several nonlinear calculations have been performed with different values of the fluid viscosity. Increasing the fluid viscosity delays and reduces the high m fluid turbulence (Fig. 4); however, the analytic calculation still predicts the correct rate of growth.

In Fig. 5, the growth rate of the (m=3, n=2) mode and voltage trace for the same nonlinear calculation are compared. It shows that the time scale of the voltage spike is the same as the anomalous growth in the last phase of the calculation and confirms the theoretical prediction of Sec. V.

In the last phase of the numerical calculation, when high $\vec{k}$ modes are being generated, a serious concern arises about the numerical validity. In going to smaller-scale lengths, more Fourier components and finer grid sizes are required, and, of course, at a certain time (for any finite number of modes and grid points) the numerical calculation breaks down. Detailed tests on numbers of modes and grid sizes are necessary to assess the reliability of the numerical results. It is convenient to do these tests for a case with $S = 10^5$. This type of numerical test has also been done in Ref. 25. That work has confirmed our numerical results,[11] and there is basic agreement on the

nonlinear numerical results presented in Ref. 25 and in the present paper. However, the physics interpretation is different.

The explosive growth phase of these calculations can be observed easily in the low m modes, like the $(m = 2; n = 1)$ or $(m = 3; n = 2)$. As stated above, the modes for which this growth is most apparent depends on the initial conditions. The relative magnitude of the initial perturbations determine the sizes of the respective magnetic islands when they overlap. These, in turn, determine the island size and sign of Δ' for these modes at the beginning of the last phase. If Δ' for the $(m = 3; n = 2)$ mode, for instance, is no longer positive at this point, the fast growth is not observed for this mode, although it can be seen for other modes. This dependence on the sign of the instantaneous Δ', strongly suggests[11] the presence of an anomalous dissipative mechanism associated with the fast growth process and confirms the present theoretical model. To present the results of the numerical tests, the $(m = 2; n = 1)$ magnetic energy has been chosen as a test mode. During the last phase (after the arrow in Fig. 6), the magnetic energy of the $(m = 2; n = 1)$ mode exhibits fast destabilization. In this case a 48 mode calculation, which gives very well-converged results fo the previous phases, is insufficient to provide reliable results. In fact, it does not show the destabilization seen in calculations with higher numbers of modes. Comparison of the results for 106 mode and 191 mode calculations (Fig. 6) show relatively good convergence up to $t = 7 \times 10^{-3} \tau_R$. In every case, we have observed that, during this phase, the inclusion of an insufficient number of modes in the calculation gives a more stable result. This could be expected from the theoretical model. To push

the calculation further in time, more and more modes are required and therefore the calculation must be stopped at a certain time (at about $t = 7 \times 10^{-3} \tau_R$ for the best converged results in Fig. 6). The magnetic energy spectrum at four times in the calculation (with 191 modes) is shown in Fig. 7. The linear dimensions of the ellipses in Fig. 7 are proportional to the logarithm of the magnetic energies of the modes in the calculation. The scale is chosen such as to show the modes having magnetic energies within five orders of magnitude of the largest value [excepting the $(m = 0; n = 0)$]. This figure clearly shows the rapid generation of high $\vec{k}$ modes in the last phase. The broadening of the spectrum indicates the need for increasing the number of modes at later times in the calculation. The comparison of the spectra at the time $t = 6.6 \times 10^{-3} \tau_R$ (Fig. 8) shows how poor the 48 mode representation is at the time when the corresponding $(m = 2; n = 1)$ magnetic energy begins to depart from the converged value.

The fast growth during the last phase of the numerical calculations depends also on the value of S. For $S \lesssim 10^4$ it is not observed, but its importance increases with S. This is consistent with the theoretical model described before. If S is small, the collisional dissipation is large, the k spectrum has only few low m modes, and consequently $\langle \phi^2 \rangle$ is reduced. At the same time, the anomalous dissipation can not be observed because it must compete with a higher level of collisional resistivity.

Finally the numerical reproducibility of this calculation has also been tested by varying the time step size. The time step ($\Delta t = 1.7 \times 10^{-7} \tau_R$) used in this highly nonlinear regime is an order of magnitude smaller than the one[24] appropriate for the linear phase of the calculation ($\Delta t \approx 1.6 \times 10^{-6} \tau_R$). Decreasing the time step below the quoted value does not change the numerical results. All the tests done exclude any possible interpretation of this fast growth as a numerial instability. We have also tested the dependence of the results on truncation error due to the finite difference radial grid. Increasing or decreasing the radial grid density by a factor of two also has no appreciable effect on the converged results in Fig. 6.

VII. CONCLUSIONS

A theory of anomalous tearing mode growth and the major tokamak disruption has been developed. The general structure and properties of the renormalized, reduced resistive magnetohydrodynamic equations have been discussed for the infinite medium and sheared magnetic field cases. For the physically relevant case of multiple-helicity turbulence in a sheared magnetic field, an anomalous ohmic diffusivity of magnetic flux by fluid turbulence was found to be the dominant nonlinear effect on a long wavelength tearing instability. A nonlinear tearing mode growth rate, $\gamma_k \sim \langle\phi^2\rangle^{3/8} \Delta'^{1/2}$, was derived. It was demonstrated that the nonlinear tearing growth and the negative voltage spike occur on roughly comparable time scales. The analytical predictions were found to be in good agreement with numerical solutions of the basic nonlinear equations.

The major unanswered question remaining is how the short wavelength turbulence is generated. An understanding of the energy flow from long to short wavelength is needed to answer this question. Such an understanding requires the construction and analysis of a renormalized energy spectrum evolution equation. Preliminary results of such an analysis indicate that a broad, slowly decaying spectrum of poloidal mode numbers is generated by the cascade of energy from long to short wavelength. Such a cascade results from the balance of vorticity damping with incoherent emission processes not treated in this paper. Furthermore, the explosive character of the disruption growth rate follows from the fact that while the low m modes feed the large m region of the spectrum, the larger m modes act in turn to provide destabilizing dissipation for low m modes. Hence, a positive

feedback loop develops. We will discuss these growth processes and the cascade mechanism in a future publication.

ACKNOWLEDGMENTS

The authors thank Professor M. N. Rosenbluth for useful conversations, and Mr. Gerald Craddock for a careful reading of the manuscript.

This research was sponsored by the Office of Fusion Energy, U.S. Department of Energy, under Contract No. W-7405-eng-26 with the Union Carbide Corporation and by Contract DOE/ET/53088 with the Institute for Fusion Studies.

REFERENCES

[1]E. P. Gorbunov and K. A. Razumova, At. Energy 15, 363 (1963) [Sov. At. Energy 15, 1105 (1963)]; L. A. Artsimovich, S. V. Mirnov, and V. S. Strelkov, At. Energy 17, 170 (1964) [Sov. At. Energy 17, 886 (1964)]; V. S. Vlasenkov, V. M. Leonov, V. Y. Merezhkin, and V. S. Mukhovatov, Nucl. Fusion Suppl. 1, 1 (1975).

[2]B. V. Waddell, B. A. Carreras, H. R. Hicks, J. A. Holmes, and D. K. Lee, Phys. Rev. Lett. 41, 1386 (1978); B. V. Waddell, B. A. Carreras, H. R. Hicks, and J. A. Holmes, Phys. Fluids 22, 896 (1979).

[3]H. P. Furth, J. Killeen, and M. N. Rosenbluth, Phys. Fluids 16, 1054 (1963).

[4]B. A. Carreras, H. R. Hicks, J. A. Holmes, and B. V. Waddell, Phys. Fluids 23, 1811 (1980).

[5]B. A. Carreras, H. R. Hicks, and D. K. Lee, Phys. Fluids 24, 66 (1981).

[6]B. A. Carreras, J. A. Holmes, H. R. Hicks, and V. E. Lynch, Nucl. Fusion 21, 511 (1981).

[7]H. R. Hicks, B. A. Carreras, and J. A. Holmes, "The effect of diamagnetic rotation on the nonlinear coupling of tearing modes" (to be published).

[8]H. R. Strauss, Phys. Fluids 19, 134 (1976).

[9]P. H. Rutherford, Phys. Fluids 16, 1903 (1973).

[10]B. A. Carreras, M. N. Rosenbluth, and H. R. Hicks, Phys. Rev. Lett. 46, 1131 (1981).

[11]H. R. Hicks, J. A. Holmes, B. A. Carreras, D. J. Tetreault, G. Berge, J. P. Freidberg, P. A. Politzer, and D. Sherwell, in Plasma Physics and Controlled Nuclear Fusion Research 1980 Vol. I, IAEA, Vienna (1981) 259.

[12]P. H. Diamond, R. D. Hazeltine, B. A. Carreras, and H. R. Hicks, Sherwood Theory Meeting, 1981.

[13]D. Fyfe and D. Montgomery, J. Plasma Phys. 16, 181 (1976).

[14]A. Pouquet, J. Fluid Mech. 88, 1 (1978).

[15]R. H. Kraichman, J. Fluid Mech. 47, 513 (1971).

[16]D. J. Tetreault, Phys. Fluids 25, 527 (1982).

[17]R. H. Kraichman J. Fluid Mech. 5, 497 (1959).

[18]E. N. Parker, Geophys. Astrophys. Fluid Dynamics 24, 79 (1983).

[19]D. Biskamp and H. Welter, Phys. Lett. 96, 25 (1983).

[20]R. H. Kraichman, Phys. Fluids 8, 13853 (1965).

[21]A. Pouquet, U. Frisch, and J. Leorat, J. Fluid Mech. 77, 321 (1976).

[22]C. E. Leith, J. Atmos. Sci. 28, 145 (1971).

[23]C. E. Leith and R. H. Kraichman, J. Atmos. Sci. 29, 1041 (1972).

[24]H. R. Hicks, B. A. Carreras, and J. A. Holmes, J. Comput. Phys. 44, 46 (1981).

[25]D. Biskamp and H. Welter, in Plasma Physics and Controlled Nuclear Fusion Research, Proceedings of the 1982 IAEA Conference, CN-41/T (to be published).

FIGURE CAPTIONS

1. The calculations are performed in such a way that the various physical effects appear as a sequence of events. (a) The radial extent of three of the magnetic islands. (b) The instantaneous growth rate of the (m=3; n=2) mode.
2. Before the final phase, the 3/2 magnetic island width evolution is effected by a sudden change in the level of resistivity (by a factor of 3). At $t = 2.27 \times 10^{-3} \tau_R$ and thereafter, the evolution becomes independent of η. For this calculation, $S = 10^6$.
3. The growth rate of the (m=3; n=2) mode as obtained from the model is compared with the calculation. Same case as in Fig. 2.
4. Same comparison as in Fig. 3, but in the presence of fiuid viscosity.
5. Same case as Figs. 2, 3: (a) Growth rate of the (m=3; n=2) mode kinetic energy; (b)Voltage trace.
6. Magnetic energy of the (m=2; n=1) mode for calculations with 48, 106 and 191 modes. Same case as Fig. 2, but at $S = 10^5$.
7. Magnetic energy spectra at a sequence of 4 times for the 191 mode case of Fig. 6. The linear dimensions of each ellipse are proportional to $\log_{10}(E^M \times 10^5/\mathrm{MAX}(E^M))$. No ellipse is plotted when this is negative ($E^M < 10^{-5}\mathrm{MAX}(E^M)$). The (m=0; n=0) mode is excluded since it would entirely dominate the picture.
8. The magnetic energy spectra at $t = 6.62 \times 10^{-3} \tau_R$ are shown for the 48, 106, and 191 mode calculations of Fig. 6.

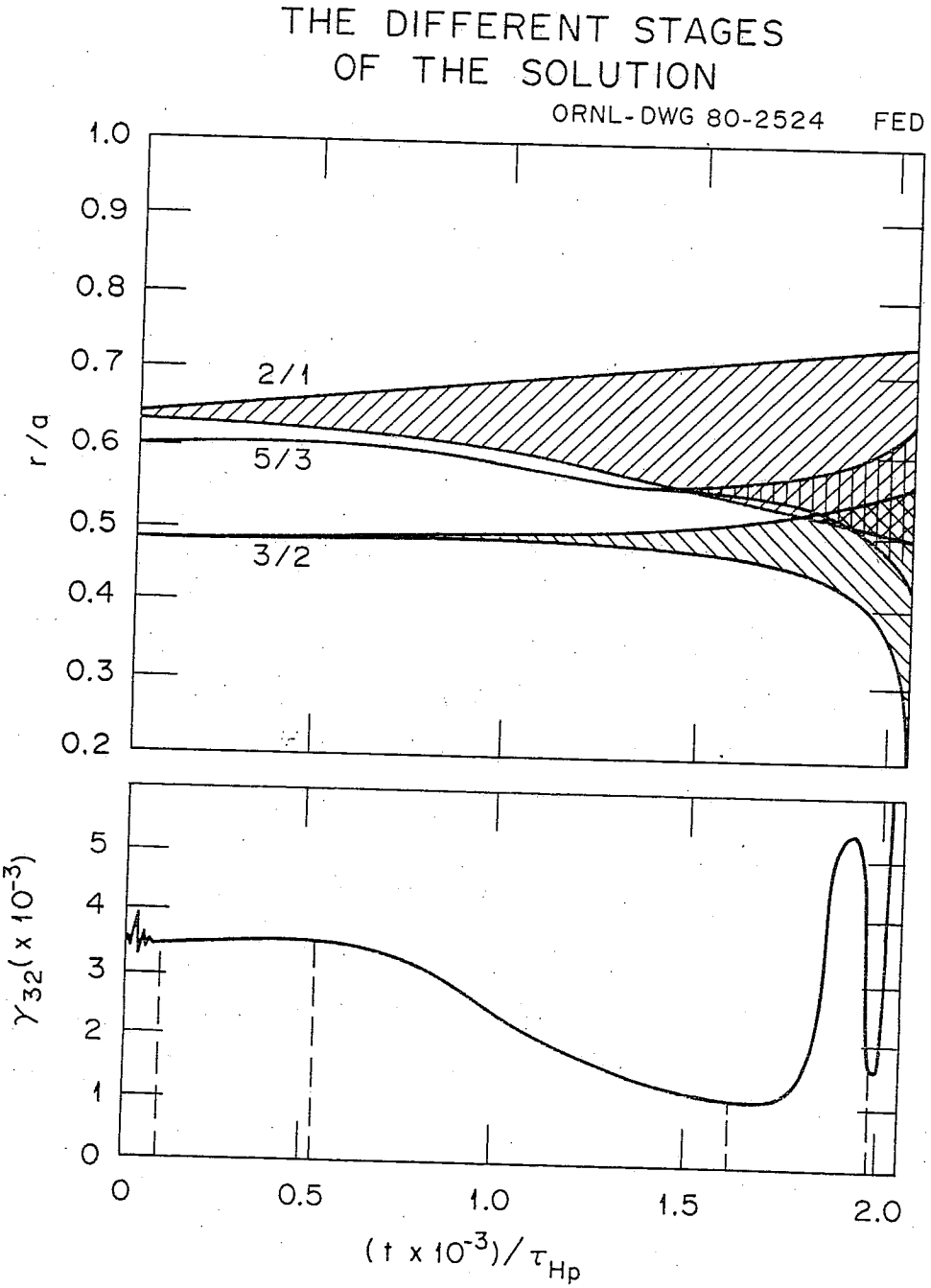
THE DIFFERENT STAGES
OF THE SOLUTION
ORNL-DWG 80-2524 FED
1.0
0.9
0.8
0.7
0.6
0.5
0.4
0.3
0.2
r/a
2/1
5/3
3/2
5
4
3
2
1
0
γ_{32}(x 10^{-3})
0
0.5
1.0
1.5
2.0
(t x 10^{-3})/τ_{Hp}

Fig. 1

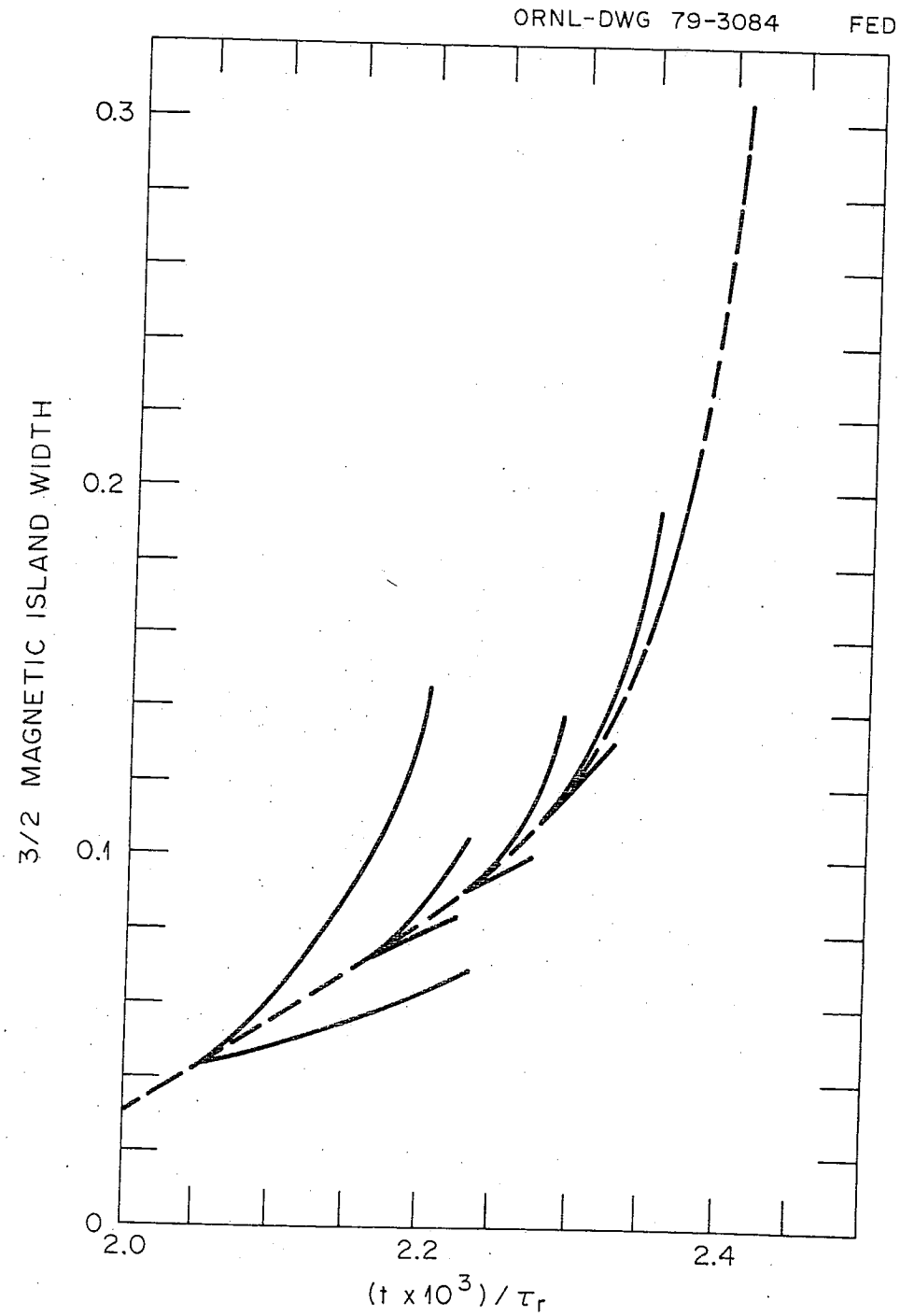
ORNL-DWG 79-3084
FED
3/2 MAGNETIC ISLAND WIDTH
0.3
0.2
0.1
0
2.0
2.2
2.4
(t x 10^3) / τr

Fig. 2

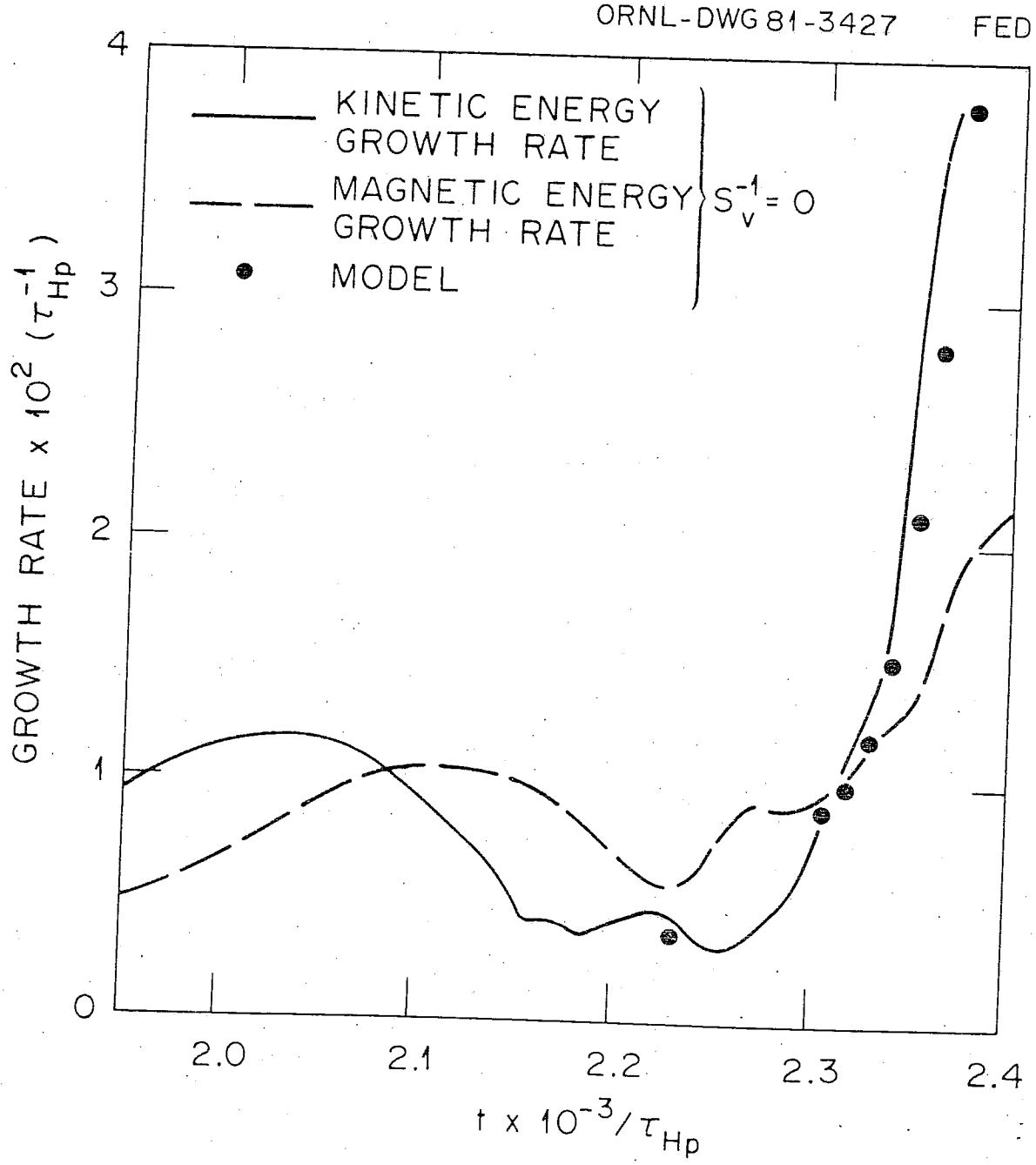
ORNL-DWG 81-3427 FED
KINETIC ENERGY GROWTH RATE
MAGNETIC ENERGY GROWTH RATE
MODEL
$S_v^{-1} = 0$
GROWTH RATE x 10^2 (τ_{Hp}^{-1})
$t \times 10^{-3}/\tau_{Hp}$
0
1
2
3
4
2.0
2.1
2.2
2.3
2.4

Fig. 3

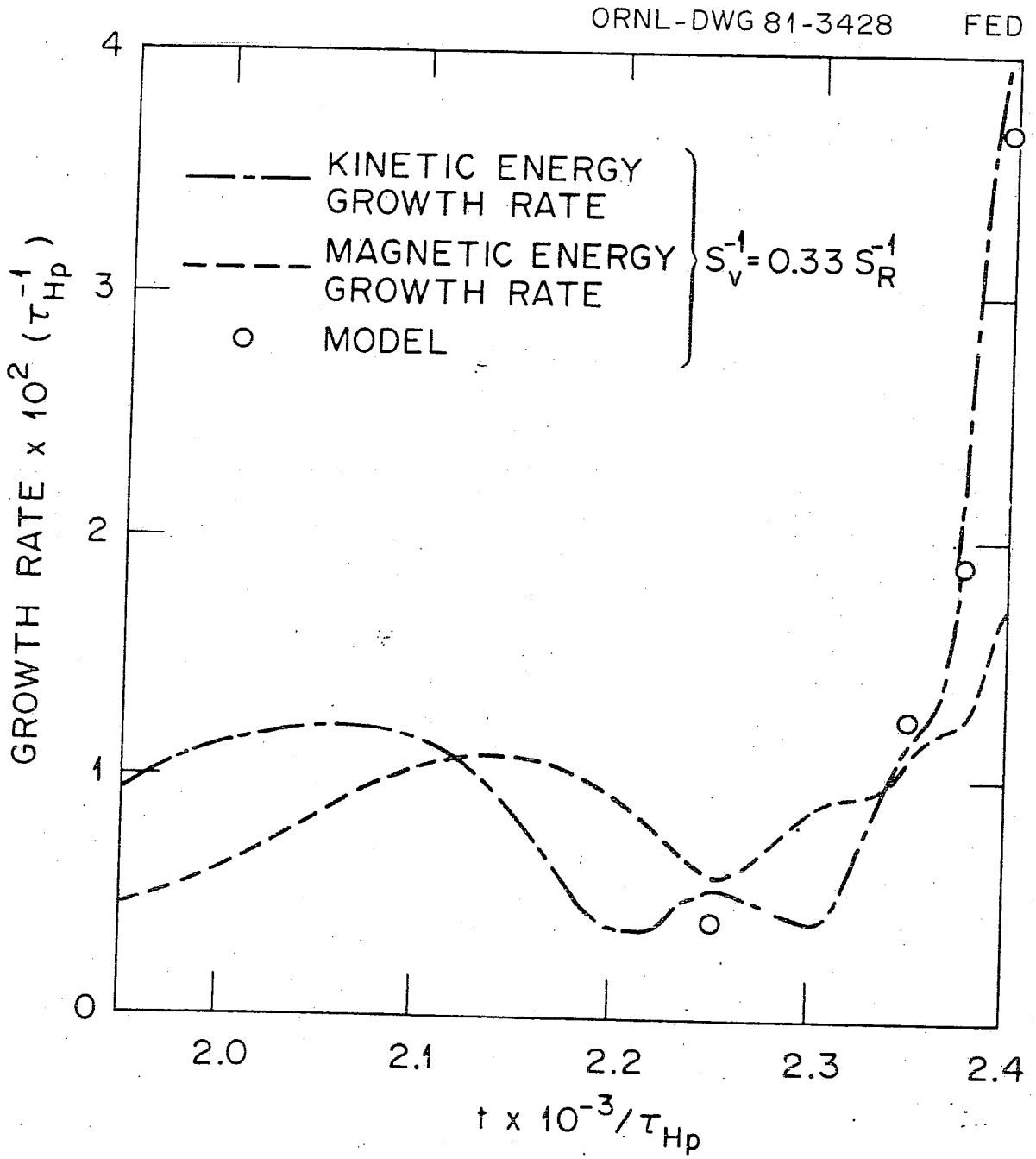
ORNL-DWG 81-3428 FED
KINETIC ENERGY GROWTH RATE
MAGNETIC ENERGY GROWTH RATE
MODEL
$S_v^{-1} = 0.33\, S_R^{-1}$
GROWTH RATE x 10^2 (τ_{Hp}^{-1})
0
1
2
3
4
2.0
2.1
2.2
2.3
2.4
t x $10^{-3}/\tau_{Hp}$

Fig. 4

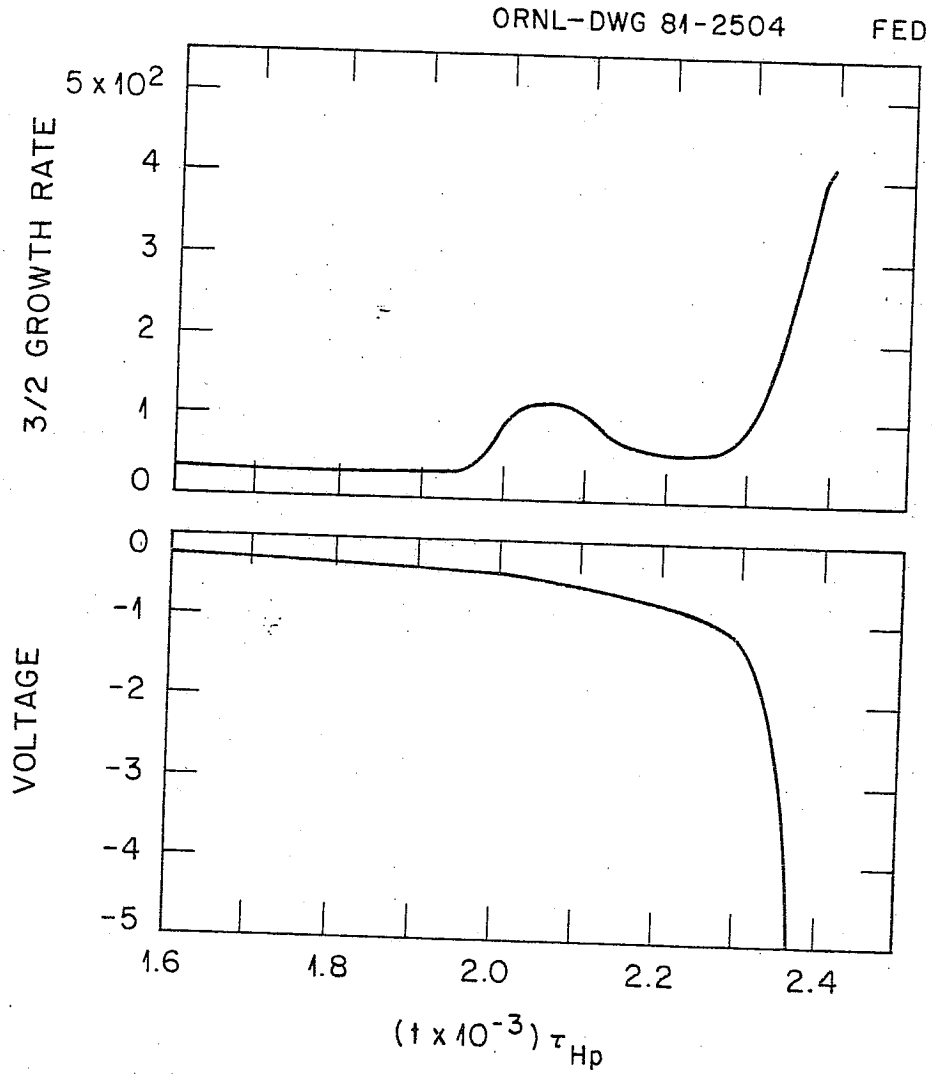
ORNL-DWG 81-2504
FED
3/2 GROWTH RATE
5 x 10^2
4
3
2
1
0
VOLTAGE
0
-1
-2
-3
-4
-5
1.6
1.8
2.0
2.2
2.4
(t x 10^-3) τ_Hp

Fig. 5

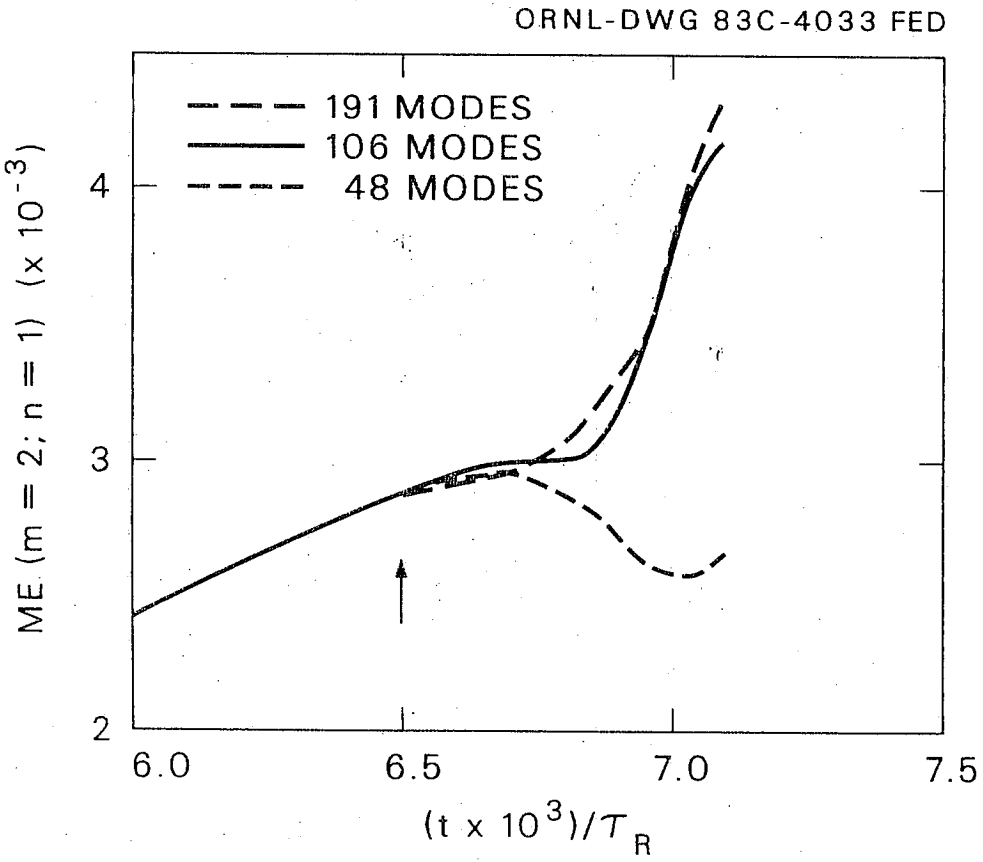
ORNL-DWG 83C-4033 FED
191 MODES
106 MODES
48 MODES
ME (m = 2; n = 1) (x 10^{-3})
4
3
2
6.0
6.5
7.0
7.5
(t x 10^{3})/τ_R

Fig.6

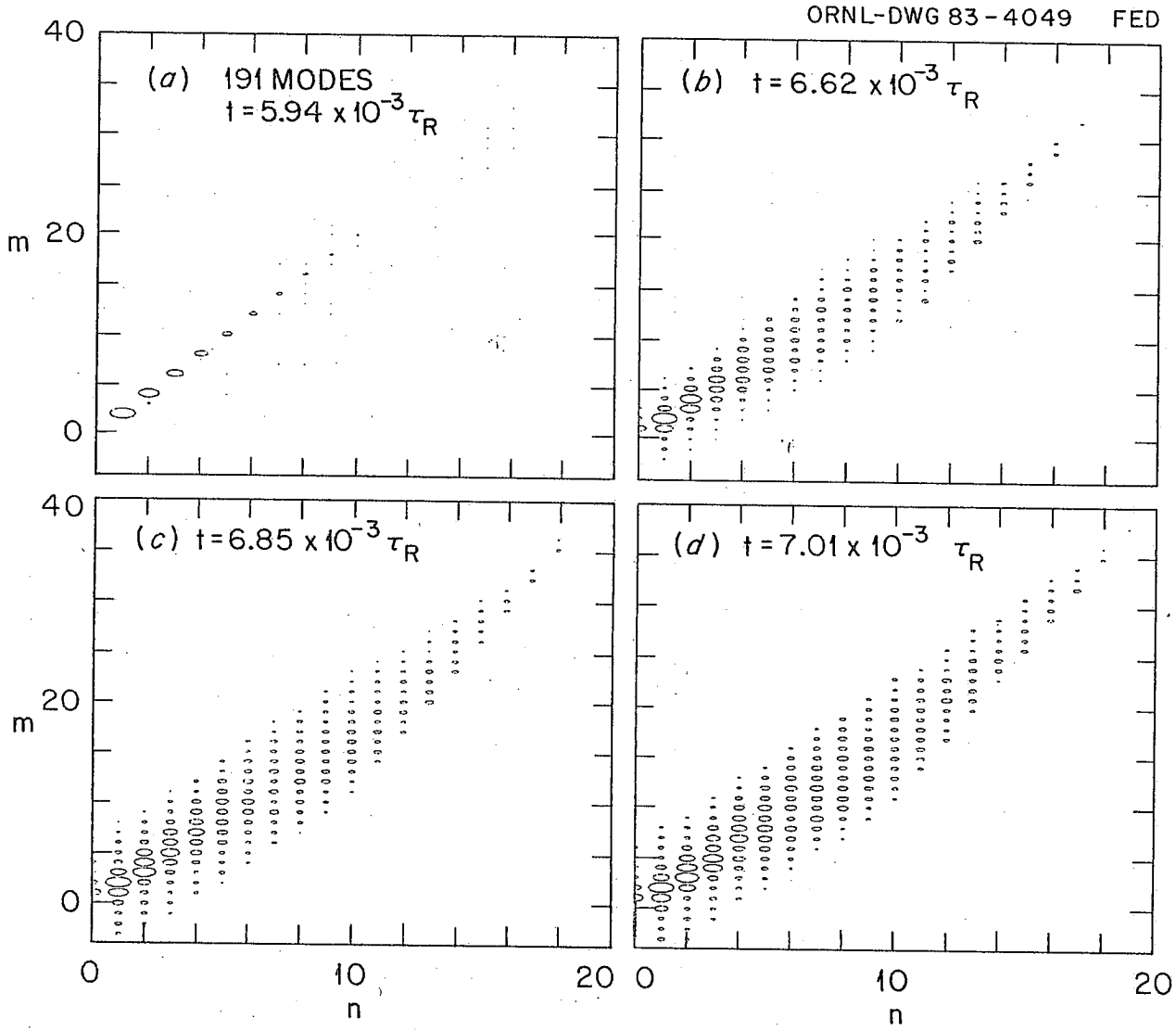
ORNL-DWG 83-4049 FED
(a) 191 MODES
t = 5.94 x 10^-3 τR
(b) t = 6.62 x 10^-3 τR
(c) t = 6.85 x 10^-3 τR
(d) t = 7.01 x 10^-3 τR
m
n
0
10
20
40

Fig. 7

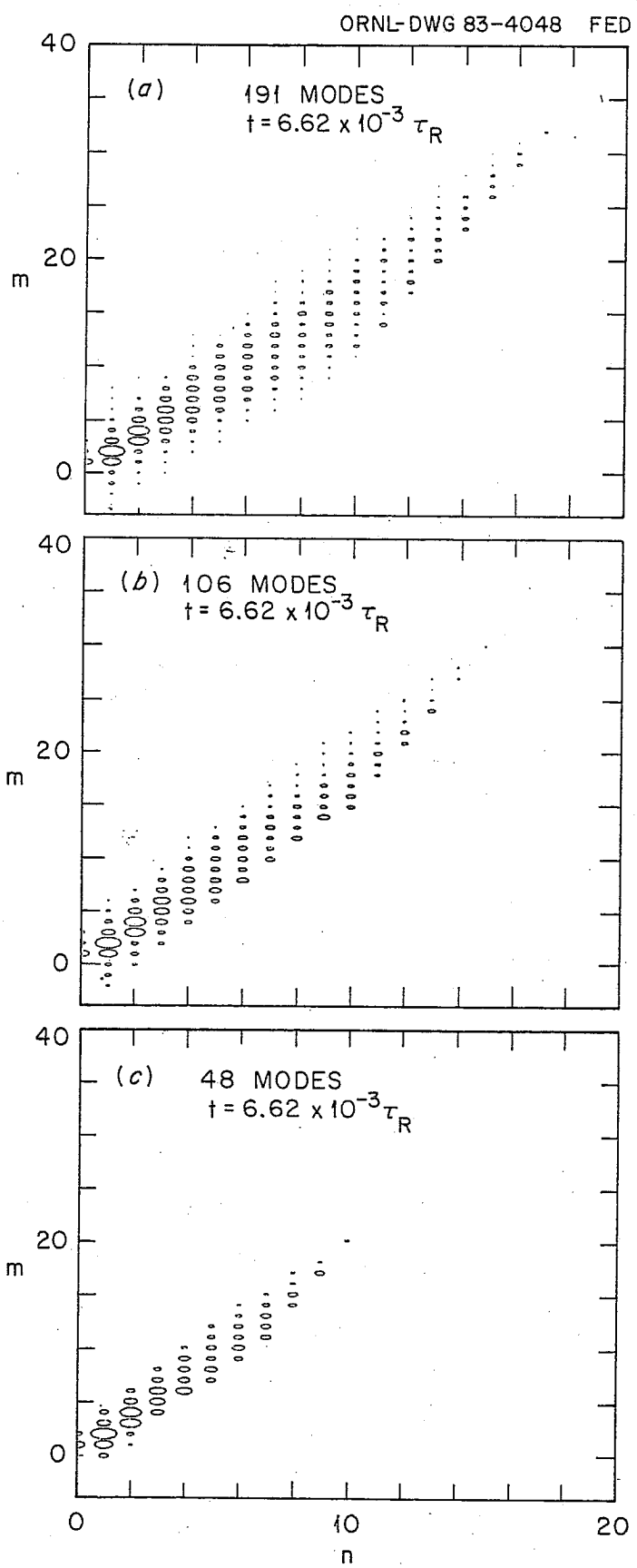
ORNL-DWG 83-4048 FED
(a) 191 MODES
t = 6.62 x 10^-3 τR
(b) 106 MODES
t = 6.62 x 10^-3 τR
(c) 48 MODES
t = 6.62 x 10^-3 τR
m
n
0
20
40
10

Fig. 8